Charles University in Prague
Faculty of Mathematics and Physics

MASTER THESIS

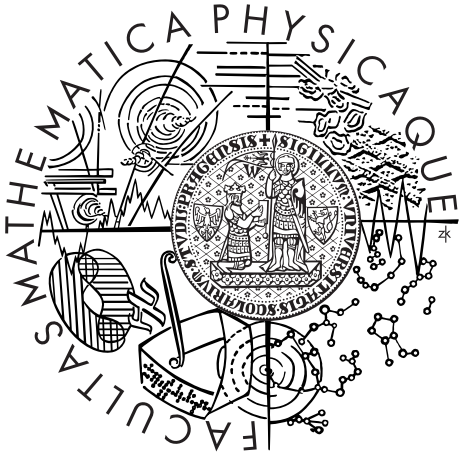

Matej Marko

Sound simulaton of granular materials

Department of Software and Computer Science Education

Supervisor of the master thesis: doc. Ing. Jaroslav Křivánek Ph.D.
Study programme: Informatics
Specialization: Software systems

Prague 2013

I would like to thank my supervisor, Jaroslav Křivánek, for being courageous and allowing me to do the thesis with a topic slightly outside the main scope of computer graphics and also for his valuable insights and advice. My family, for their never ending mental and financial support. My friends, for being there for me. At last, I would like to thank the members of The Buckets and The Elizabeths, for tolerating my, sometimes wicked, musical ideas.

I declare that I carried out this master thesis independently, and only with the cited sources, literature and other professional sources.

I understand that my work relates to the rights and obligations under the Act No. 121/2000 Coll., the Copyright Act, as amended, in particular the fact that the Charles University in Prague has the right to conclude a license agreement on the use of this work as a school work pursuant to Section 60 paragraph 1 of the Copyright Act.

In ..... date ..... signature of the author

Název práce: Simulace zvuku sypkých materiálů
Autor: Matej Marko
Katedra: Kabinet software a výuky informatiky
Vedoucí diplomové práce: doc. Ing. Jaroslav Křivánek Ph.D., Kabinet software a výuky informatiky

Abstrakt: V posledních letech byly vyvinuty metody pro simulaci zvuku pevných těles, tekutin, ohně a tkanin. Tyto metody jsou rozšířením existujících metod pro vizuální simulaci jednotlivých jevů, ke kterým přidávají fyzikálně založené zvuky, korespondující s vizuálními výsledky. Cílem této práce je prozkoumání možnosti vyvinout podobnou metodu pro sypké (zrnité) materiály. Identifikovali jsme dvojici mechanismů, které se podílejí na zvuku sypkých materiálů: kolize mezi částicemi sypkého materiálu a kolize mezi částicemi a okolními pevnými objekty. Navrhli jsme metodu, která modeluje zvuk kolizí částic jako akcelerační šum. Částice jsou aproximovány koulovým tvarem. Zvuk kolizí mezi částicemi a pevnými objekty simulujeme pomocí metody modální analýzy. Jelikož většina metod pro vizuální simulaci sypkých materiálů neposkytuje informaci o kolizích, prezentuje taktéž způsob jak tyto kolize náhodně generovat.

Klíčová slova: simulace zvuku, sypké materiály, modální analýza

Title: Sound simulation of granular materials
Author: Matej Marko
Department: Department of Software and Computer Science Education
Supervisor: doc. Ing. Jaroslav Křivánek Ph.D., Department of Software and Computer Science Education

Abstract: In recent years, methods for simulating sounds of solid objects, fluids, fire and cloth have been developed. These methods extend existing methods for simulation of the visual behaviour of the respective phenomena and add physically based sounds that correspond with the visual information. The goal of this thesis is to investigate the possibility of creating a similar method for sound simulation of dry granular materials. We identified two distinct mechanisms responsible for the sounds of granular materials: the collisions of the particles of the granular material (**granular collisions**) and the collisions between the particles and a surrounding solid objects (**solid objects collisions**). We propose a method that uses acceleration noise to simulate the sounds of the granular collisions. The particles are approximated by a simplified spherical shapes. We also simulate the sound of the solid object collisions by using a modal analysis approach. Since most of the approaches to the visual simulation of granular materials do not provide the information about the particle collision, we also present a probabilistic approach to random generation of collision data.

Keywords: sound simulation, granular materials, modal analysis, acceleration noise

Contents

1. Introduction

The world around us provides an enormous amount of phenomena that we perceive through our senses - images, sounds, smells to name a few. They have always caught people's imagination. It seems that it is in the human nature to try and capture the surrounding world. For example, most of the children spend long hours drawing or painting images and for centuries visual artists perfected their technique in order to catch every detail. This effort doesn't end with an imitation. We often use perceived sensations to trigger our imagination and create something new. An abstract painting, a poem or a song.

Technical innovations not only makes our life easier, they also provide new ways to recreate the world. First it was the photograph that allowed us to capture a static visual information. Then the sound recording gave an opportunity to record a sound and play it again when needed and the video recording made it possible to preserve a dynamic visual information. More recently, the invention of digital computers brought unprecedented opportunities for capturing the world. Data, such as sounds or videos, can be stored digitally and processed more rapidly and easier then before.

The use of computers is not only limited to work with the data obtained by observing a real environment (sounds, images, videos, etc.). There is also a possibility to create similar data from a digital simulation of the environment. In general, we can say that we are creating virtual environments. These virtual environments include computer games, visual effects in movies, commercial product visualisations, etc.

For example, imagine a photograph of a real world street. It displays a road and a series of buildings. We can produce a digital version of such a street by creating 3D models of the buildings and textures that mimic the appearance of the buildings. When the digital version is available, we can use a rendering algorithm (see for example Book [40]) and produce image similar to the photograph.

Similar approach can be used for videos and sounds as well - create digital description of the phenomena, simulate and observe results. In music industry, it is common to use digital versions of musical instruments[1]. An artist writes his or her musical idea into notes and feeds the notes into a recording software, which is capable of running virtual instruments. The chosen virtual instrument creates a sound that is from that moment treated in the same way as if it has been recorded on a real instrument.

However, virtual musical instruments are a specific category in sound simulation. In the majority of the virtual environments the sound sources are various physical phenomena (e.g. collisions of the solid objects, running water, footsteps, etc.) For impressive experience, it is necessary that the sound corresponds with the perceived visual sensation. So far, this correspondence relied heavily on the work of foley artists.

For a certain phenomena, the correspondence of audio and visual sensation is easily achievable by playing prerecorded sound at the right moment. This include discrete events, such as collisions of solid objects or ringing of a doorbell.

[1]The Reader may refer to the website `http://www.vst4free.com/` for a collection of free virtual instruments and effects.

However, when dealing with a physical simulation or an interactive process, it is much more difficult. Take for example a animation of the water. Each time a visual artist changes the animation, a foley artist must adapt the sound. In the worst case scenario, the new version of animation differs from previous to such extent that the foley artist must start his work all over again. It is clear that the methods that produce sound according to an animation are desirable. Even if the resulting sound is not artistically fine according to a director, a foley artist can still use it as a base for his work and further enhance it.

The visual quality of the virtual environments is always improving[2] and so should be the quality of sound. Simulating the reality to the last atom is not feasible with the computation power of current computers. Therefore, it is necessary to create methods that are specialised to a limited number of scenarios and thus effective.

1.1 Motivation

In recent years, multiple techniques for animation of granular materials have been developed (see Articles [56], [34], and [20]). These methods provide a way to simulate the behaviour of granular material with sufficient and realistic visual results.

Similarly, physically based (or physically inspired) sound simulation has made a rapid progress. The main focus has been on research of sounds produced by interactions of solid objects (see for example [52], [35], [37] or [10]). However, other sound producing phenomena have been investigated as well: flames [11], cloth [2] and water [54], [33]. These methods are designed to extend (or use) existing methods for animation of the respective phenomena and produce the sound, which corresponds with the animation.

Sound produced by granular materials has attracted only limited attention from researchers. To our best knowledge, there is no general method for simulating sounds produced by the movement of the granular material that is controlled by the visual simulation[3]. With the existence of method for animation of granular materials, it would seem natural to try to fill this gap and investigate the possibilities of creating such a method. We hope that this thesis will be a first step in this direction.

Granular materials in movement can produce wide variety of sound. This include also some unusual phenomena such as “squeaking” or “booming” noise (see for example Article [47] or Online source [49]). We consider these to be very specific and in some cases the reasons for occurrence of this phenomena are unclear. We focus on the sounds produced by a relatively small amount of dry granular material with particle size in the order of millimetres (for example sugar, sand or gravel).

[2] As an example, look at the visuals of any modern AAA computer game or the visual effects in any action blockbuster.

[3] There are some method focused on certain scenarios. See Section 1.4.4, for more details

1.2 Organization

This thesis is organised as follows. In the remainder of Chapter 1, we briefly present previous work that is related to our research. In Chapter 2 we introduce basic concepts from the fields of sound simulation and granular materials. We do not intend to provide full explanation, we cover only topics necessary to understand decisions and reasoning in this thesis. However, we pay more attention to the ideas that are used extensively in our research. In Chapter 3 we present method for simulating sound produced by vibrations of solid objects and in Chapter 4 we introduce the concept of acceleration noise.

In Chapter 5 we present the developed method for sound simulation of the granular materials. The results achieved by this method are presented in Chapter 6. We conclude the thesis and discuss possibilities for future work in Chapter 7.

The thesis also contains number of appendices. Arguably, the most important is Appendix B that discusses the sound samples. It contains the description of recording process for the real world experiments, as well as the description of the scenarios used in digital simulations. It also contains list of the sound samples.

1.3 Sound samples

This thesis is accompanied by a number of sound samples. These samples include recordings of the real world experiments as well as the digitally synthesised sounds. The list of the sound samples, together with the description of the recording and simulation process can be found in Appendix B.

Moreover, the sound samples are referenced throughout the thesis. In the electronic version of this text, each reference to any sound sample is accompanied by a link that tries to play the sound sample in the native audio player. Unfortunately, such a luxury is impossible to achieve in printed version. Therefore, we encourage the reader to use the electronic version of the thesis, which is located on the included CD.

1.4 Related work

1.4.1 Sound simulation - solid objects

We perceive a great deal of information about the world from the sound. It is natural that sound simulation must be an integral part of every virtual environment (e.g. a computer game or a CGI animation). Despite this fact, physically based sound simulation methods that can be used in virtual environments started to appear only a little over a decade ago.

We believe this is mainly due to the fact that sound can be prerecorded and played when needed. The technique of using prerecorded sound samples is simple, yet in most cases, it provides sufficient results. Moreover, the prerecorded samples can be further processed and enhanced by sound engineers. The clear disadvantage of using a prerecorded samples is the fact that samples are static. Once recorded and processed, they remain the same each time being played.

The majority of the work in sound simulation focused on the sound produced by vibrations of solid objects. The vibrations are typically caused by the contacts

among the solid objects. This is understandable, since contacts of solid objects are the most common sound source. In 1992, Takala and Hahn [48] presented a framework for producing soundtracks for animations. They also solve the problem of sound wave propagation using a sound-tracing approach which finds major paths between a sound source and a microphone. This approach is very similar to the path-tracing algorithm used in rendering.

Gaver [16] and [17] presented a method for synthesizing sounds produced by vibrating solid objects. This method is generally known as modal synthesis (modal synthesis is explained in Section 3.3). It models the sound produced by a solid object as a sum of multiple components called modes. Modal synthesis was also used by van den Doel et al. in Article [52]. They successfully used this method for producing not only the sounds of collisions but also for the sounds of objects rolling and scraping against each other. Parameters for the modal synthesis, which define the modes of an solid object, can be found using various techniques. Gaver [17] introduced multiple heuristics. Van den Doel et al. [52] suggested that tuning by ear can be used and Pai et al. [38] presented a method for experimental extraction of the modal data.

Direct modelling of the vibrations was introduced by O'Brien et al. [35], who modelled a solid object using finite elements method and directly integrated the movement of the object's nodes (i.e. the vertices in the object's representation). The same modelling technique was also used by O'Brien et al. in a later Article [37]. However, instead of directly integrating the movement of the nodes, they used modal analysis to extract object's modes. For more details about modal analysis, see Section 3.3.

Since then, modal analysis has been used regularly when dealing with sounds of solid objects. James et al. [22] used modal analysis as a tool in their approach. In the pre-process, they solve the sound wave propagation problem. The resulting sound field of each mode is then approximated by multiple simple sound sources. The simple sound sources are then used during the real-time synthesis instead of the original object. Raghuvanshi and Lin [42] modelled solid objects using a spring-mass system. The model is then subjected to modal analysis. They also provide multiple speed-up methods. Among them is a perceptually based method for reduction of the number of nodes. It uses the fact that humans are unable to distinguish frequencies close to each other.

Chadwick et al. [10] presented method for synthesising sounds of thin solid objects (plates, cymbals, etc.) using a non-linear coupling of the modes. Modal analysis and synthesis have been introduced also to the game programming community (see Book [26]). For the state of the art results achieved using modal analysis technique, see Article [55] by Zheng and James.

1.4.2 Acceleration noise

Acceleration noise is sound produced by solid object subjected to sudden acceleration. An accelerated object creates a disturbance in the air that is perceived as sound. As such, it complements the sounds of vibration solid objects. Although this concept is new to the sound simulation community, it has been previously studied in noise control (see Article [44]).

Koss and Alfredson [25] derived and experimentally validated a closed form

formula for acoustic pressure of acceleration noise caused by collisions of two elastic spheres. This approach is explained in Chapter 4. Later, Koss [24] used similar approach and introduced formula for inelastic spheres as well. More recently, Mehraby et al. [29] compared experimental results, analytical results provided by Koss and Alfredson [25] and simulation using finite elements method.

Chadwick et al. [13] introduced the concept of acceleration noise to the sound simulation community. They stated that acceleration noise is important for the small objects, since the frequencies of their vibration modes are often outside the audible range. They precomputed the acceleration noise of solid objects for linear and angular acceleration in the individual axes. The precomputed acceleration noise is used as a database for acceleration in arbitrary linear and angular direction. Chadwick et al. [12] used ellipsoidal proxies instead of real shapes of small solid objects, thus reducing the memory consumption and avoiding the pre-computation step.

1.4.3 Other sound simulation methods

Apart from the sounds produced by the vibrations of solid objects, other sound producing phenomena has been studied as well. Among them we can find: water, flames and cloth.

The mechanism behind the sounds produced by water (or other fluids) was identified by Minnaert as early as 1933 (see Article [32]). He claimed that sound produced by water in motion is caused by vibrations of the small air bubbles that are brought under water. For more information, refer to Book [27]. Van den Doel used the mechanism of vibrating air bubbles in Article [15] and constructed stochastic approach to simulate sounds of running water. He demonstrated his approach by creating an algorithm that allows control over the stochastic creation of the bubbles.

More recently, Zheng and James is Article [54] and Moss et al. in Article [33] showed two automated approaches for generating sound from a fluid simulation. Both methods use the fluid simulation as a trigger to produce air bubbles which are the sound producing phenomenon. Zheng and James solved also the sound wave propagation problem, whereas Moss et al. focused on real-time sound simulation.

Chadwick and James successfully extended fire simulation to produce sound [11]. The method uses the dynamically changing surface of the visual flame as a sound source. However, it is feasible to run the flame simulation only at low frequencies. Therefore, Chadwick and James provided a technique for spectral bandwidth extension to create missing high frequencies. An et al. [2] developed a technique for simulation of sounds produced by cloth in motion.

1.4.4 Sound of granular materials

There have been only a limited attention to the sounds produced by granular materials. Perry R. Cook in Article [14] presents a set of methods for physically based (he uses the term "physically inspired") synthesis of percussive instruments. Among the instruments in [14], we find a simulation of maracas. Maracas is a popular musical instrument, originally from Latin America. It is formed by a cas-

ing filled with a small amount of granular material. When shaken, the particles of granular material inside the instrument produce a typical sound. Cook simulated the movement of particles and collected collision statistics. In particular, he discovered that the waiting time between collisions can be approximated by a Poisson process.

Figure 1.1: Wooden maracas (image source `http://meinlpercussion.com/`).

Using the statistics, collisions for each shake of a virtual instrument can be randomly generated. Cook [14] suggested using various methods for synthesising the sounds, including prerecorded sound of a collision between a particle and the casing, decaying sinusoidal functions or a noise function.

Sound of the granular materials has been also investigated in terms of simulating footsteps sounds on surfaces such as sand or dirt (see [50], [31]). Luciani et al. [28] investigated sound of a piling sand. In a pile of sand, they identified three layers:

- Bottom layer - the particles are packed close together, so they resemble a block of elastic matter. Acoustically this layer act as one vibrating structure.
- Intermediate layer - the particles are still close to act like a vibrating structure, but collisions among the particles occur as well.
- Top layer - the particles that fall and collide with intermediate layer, thus exciting it.

Luciani et al. [28] implemented the method using GENESIS software (see [9] for details about GENESIS). However, they don't give the implementation details.

We must stress that the methods presented by Cook [14], Mehta [31] and Turchet et al. [50] study only very specific scenarios. Method of Luciani et al. [28] is derived by studying results of a visual simulation of granular material. They report that the method is capable of producing various phenomena associated with the sound of sand. However, the information whether the sound model can be driven by the results of visual simulation and thus automatically synthesise sound of piling sand is missing.

1.4.5 Animation of granular materials

Various approaches for visual simulation of granular materials have been developed. In this section, we only list the methods relevant to our work. More detailed description can be found in Section 2.4.

In general there are two ways of simulating the visual behaviour of granular materials: discrete approach and continuum approach. Bell et al. [5] and Alduán et al. [1] used discrete non-spherical shapes to model the particles. The continuum approach has been first presented by Zhu and Bridson [56], who model the granular materials as a fluid. The continuum approach has been extended with two-way coupling between granular material and solid objects by Narain et al. [34]. More recently, Ihmsen et al. [20] presented framework that uses smoothed particle hydrodynamics method (SPH) to simulate granular material.

2. Theoretical background

In the following sections we provide theoretical background and introduce terms that will be used in the rest of the thesis. We don't intent to thoroughly explain the details, but rather present the basic concepts.

2.1 Acoustics

Sound is the subject studied by acoustics - the science of sound. From the viewpoint of acoustics, sound is any wave motion in gases, liquids and solids [21]. This definition is general and fits many phenomena. Among them we can find:

Sound in the human hearing range

In other words, wave motion in the media around us (most often air) with frequencies inside the audible frequency range. Although, the range of audible frequencies is a matter of each individual, the range between 20Hz and 20kHz is widely recognised as an approximation for human beings. This category contains what is usually understood as "sound".

Commonly known example is a speaker reproducing a prerecorded sound. The membrane of the speaker vibrates according to the input signal and moves the air molecules in its vicinity. These molecules interact (i.e. collide) with more distant molecules and the movement propagates through the air. Due to the movement of the molecules, the pressure, density and temperature of the media changes [21]. Since human hearing organs allow us to detect only the changes in the pressure, the pressure is the quantity we are interested in. The difference between the instantaneous value of the pressure and the static pressure is called acoustic pressure (or sometimes sound pressure).

We have mentioned that air is the most common medium in which sound waves propagate. However the same principle holds for all the fluids (that being either gases or liquids) [21]. This fact is easily observable, as humans can hear under water.

Ultrasound

Ultrasound are oscillations in the media around us with frequencies higher than the audible range. Sonography is a medical diagnostic technique that uses ultrasound waves to obtain images of internal body organs. In nature, bats use ultrasound waves to navigate during their flight.

Infrasound

Infrasound, when compared to ultrasound, is on the other end of the frequency range. Infrasound is formed by waves with frequencies below 20Hz. Such waves are produced by natural phenomena (e.g. earthquakes, avalanches), by animals (whale songs) or by human-made processes (explosions).

Vibration of solid objects

Vibrations of solid objects are a very common sound source, therefore it is an important subject of study in acoustics. We encounter sounds produced

by solid objects every day: a knock on the door, a spoon dropped on the table, a vibrating string on a guitar or the above-mentioned example of a speaker reproducing prerecorded sound.

2.2 Sound simulation process

The goal of the sound simulation process is to determine the value of acoustic pressure at a given location during a given time period. It is implicitly expected that there is a process that causes changes in the pressure. Otherwise, we are left with a zero pressure change (i.e. silence). The whole process is complex and can be divided into the four stages, as depicted in Figure 2.1.

Figure 2.1: The sound simulation process can be split into four stages.

Each of these stages forms a separate set of problems to be solved. The division is conceptually same as the one presented by van den Doel in Thesis [51] (see Figure 2.2). However, in Thesis [51] only the sounds produced by contacts of solid object are studied. Therefore, the first stage is separated in two distinct steps: impact and vibration. We use more general first stage. As a result, variety of sound sources can fit in. In the remainder of this section we briefly explain the stages and try to illustrate them with a few examples.

Figure 2.2: The idea of dividing the sound simulation into five separate stages is presented in Thesis [51].

In the first stage we must identify the sound source and simulate the mechanism that produces the sound waves. For example, when simulating sounds of contacts of solid objects, we need to simulate movement, collisions and vibrations of these objects. Simulation of sounds produced by fluids involves the fluid simulation itself.

The second stage is concerned with the emission of the sound waves from the source to the air (or other medium). For solid objects it solves the question: "What happens on the interface between an object and the surrounding medium".

As the sound wave propagate from the sound source further away, it may encounter other object in the environment and phenomena such as reflection, absorption, scattering and diffraction (see [21]). Note that these are not dissimilar to the problems solved in photo-realistic rendering. The third stage solves the propagation of the sound waves in the environment. This is achieved by solving the linear wave equation (Eq 2.1, see [21], [23]). It can be said that this stage solves the relationship between a sound source at position A and the value of acoustic pressure at position B.

$$\nabla^2 p = \frac{1}{c^2}\frac{\partial^2 p}{\partial t^2} \tag{2.1}$$

The last stage is concerned with a listener, which is almost exclusively a human. Humans have a pair of hearing organs, located at the opposite sides of the head. As a result of this, the sound wave reaches each ear at a different time. This time difference is crucial for locating the position of the sound source. Hearing organs are also responsible for spectral filtering of the incoming sound waves. This is modelled by head related transfer functions (HRTF) (for more information, see for example Book [4]).

To obtain physically correct results, it is necessary to address all of the stages. However, it is important to note that for a certain situation, compelling results can be achieved by using only an approximation or even completely omit some of the stages. For example, in interactive virtual environment (such as a computer game), strict time budget doesn't allow any computationally extensive simulation. However, playing prerecorded samples and applying spatialization effects is a sufficient solution.

2.3 Everyday listening

"**Everyday listening**" is a term defined by Gaver in Article [18] as "hearing the events in the world rather than sounds per se". It means that we are used to identify the sounds we perceive with the situations that produce them. For example, when two solid objects collide, a listener is not concerned with the spectrum of the sound. He uses his previous experience and associates the sound with the materials and size of the objects.

According to Gaver [18], opposed to everyday listening stands "**musical listening**". In musical listening we are concerned with properties of the sounds such as pitch, spectral characteristics (usually called timbre) and rhythmical properties. The difference between every day and musical listening can be illustrated on an example of a listener hearing a guitar playing. Everyday listening description is: "there is someone loudly playing a guitar in the neighbouring flat". Whereas musical description says: "I hear a guitar playing Rumble by Link Wray, but the rhythm is wrong".

We can find analogy of everyday and musical listening in sound simulation. Virtual musical instruments and effects are concerned with musical characteristics: the pitch must be perfect, the timbre must be as close to the real instrument as possible. The goal of general sound simulation is to provide sound information about the virtual environment (e.g. a material of a sounding object).

2.4 Granular materials

Granular materials (or granular media) are commonly found both in nature and among human-made products: sand, gravel, soil, salt, sugar, flour, ball bearings, etc. These materials are composed of great amount of small, rigid objects (particles or grains). The interactions among the particles give these materials

unique properties on the macroscopic scale. Behaviour of a granular material can resemble solids, liquids or gases as well [30].

For example, imagine a pile of sand. When it is in equilibrium, it acts similarly as a solid. Although the gravitational forces are applied, the shape of the pile remains unchanged. However, when the pile is disturbed from the equilibrium state, it starts to flow like a liquid. Add a wind to the scenario and if the wind is strong enough, it picks up the sand grains and creates a dust. Note that, gas-like behaviour is more easily observable in the granular materials with very fine grains (flour, powdered milk, etc.). Such materials are called powders.

2.4.1 Simulation of granular materials

In this section we briefly review the methods for simulating granular materials. We emphasise that this is not a exhaustive review of simulation methods. We mention only the methods relevant to our work in sound simulation of granular materials.

Methods for simulation of granular materials can use either a discrete or a continuum approach. In the discrete approach, the material is simulated using discrete elements that represent the individual grains. The movement and the interactions of the elements are explicitly simulated.

To capture the properties of the granular materials, Bell et al. in Article [5] use non-spherical elements (particles) to represent the grains of the material. The non-spherical shapes of the particles are able to produce phenomena such as piles of the material [5]. They use the shapes compounded from multiple smaller spherical shapes. These compound particles approximate the grains with more complex shapes. See Figure 2.3 for approximation of a tetrahedron and a cube.

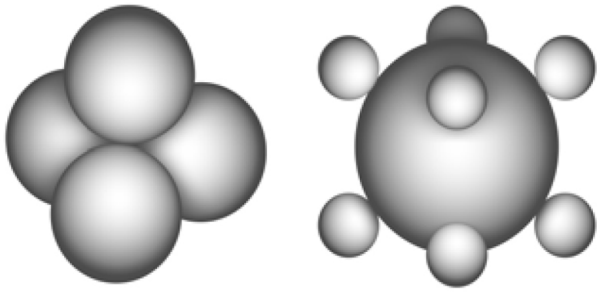

Figure 2.3: Non-spherical compound shapes used to represent grains in Article [5]. Displayed shapes are approximation of tetrahedron (left) and cube (right).

In Article [5], Bell et al. also present a method for efficient collision detection among the particles and a way of interaction between the granular material and rigid bodies. To incorporate rigid bodies, they extend the idea of using the compound shapes for the grains of the material. The surface of a rigid body (given by a triangle mesh) is approximated by collection of smaller spherical shapes (surface particles), thus forming one complex compound shape. By simulating the surface particles together with the particles of granular material, they achieved two-way coupling between the granular material and the rigid bodies [5].

Alduán et al [1] argue that internal forces (i.e. the forces that arise from the interaction among the grains) need fine temporal resolution of the simulation. On the other hand, external forces (gravity or collisions with rigid bodies) require fine spatial simulation scale. To solves this problem efficiently, they extend approach presented in Article [5]. They use non-spherical particles to compute internal forces. However, the non-spherical particles are used only as low resolution guides. Internal forces are then upsampled and assigned to the high resolution particles. External forces are computed for both the LR guides and HR particles.

The number of LR guides is smaller than the number of HR particles (2500 and 50000 were used in one of the examples presented in Article [1]). Therefore, the computation of internal forces is efficient. The external forces are computed also for the HR particles. As a result, fine spatial resolution is achieved.

Interesting way of simulating the granular materials comes in a form of event-driven particle simulation. Event-driven simulation (also known as discrete event simulation) provides an alternative approach to the more common time-stepped simulation (continuous simulation). Time-stepped simulation is updated in the regular time steps and from its nature it may miss events that occur in-between the update steps.

On the other hand, in an event-driven simulation it is known when the next event occurs and the simulation can be advanced to this time. The resulting advantage is that within one update the simulation can advance the time equal to multiple time steps of the time-stepped simulation. Event-driven particle simulation can be used to study molecular dynamics, fluids or granular materials. For more information about event-driven particle simulation, refer to Article [3] that presents Dynamo[1] event-driven simulator.

It is clear that the discrete approach is limited by the number of grains that is feasible to simulate. In other words, it doesn't scale well with the increasing amount of the granular material. When using the continuum approach, the grain size and the simulation resolution are decoupled from each other [20].

With the absence of the individual grains (which is the very point of the continuum approach), two problems arise in the simulation of granular materials. Internal forces have to be found and material must be moved accordingly to the both external and internal forces (this is called advection). The forces are computed by solving an equation that controls the flow of the material. In each step the equation is solved either on a grid or using a Smoothed Particle Hydrodynamics (SPH) method. For more information about flow equation and advection, refer to Book [7].

Zhu and Bridson in Article [56] present a method for animated sand, based on a method previously used for fluid animation. The method uses a grid for computation of forces and particles for advection of the material. Narain et al. [34] use similar approach and achieve two-way coupling between the material and solid objects. It is important to note that the particles in this method are used only for advection of the material and there is no collision detection for these particles. The particles don't represent the individual grains of the material, but rather larger chunks of the material. Such an approach exploits the fact that advection is easier to solve using particles than using a grid [56].

Ihmsen et al. [20] use an approach similar to Alduán et al. [1] and split the

[1]Dynamo is an open-source event-driven simulator: `http://dynamomd.org/`

computation of internal and external forces. Internal forces are computed using the smoothed particle hydrodynamics (SPH) method and then upsampled for the high resolution particles used for advection and external forces computation. The forces applied to HR particles are blended from the sampled internal forces and computed external force (see [20]).

3. Sound simulation of solid objects

When a solid object is subject to an external force (e.g. a collision with an other object), its surface starts to vibrate. These vibrations are very small in displacement and therefore invisible to naked eye. However, they are significant enough to move the molecules of the surrounding medium (most often the air) and thus produce pressure changes in the medium. If the pressure changes have frequencies in the audible range (widely recognised as 20Hz to 20kHz), we perceive the vibrations as sound.

It is clear that the collisions of solid object are one of the most common sound sources [18]. Such sounds appear around us everyday. Vibrations of an object are affected by its shape and material. Therefore, the sound produced by a collision of two solid objects reveals a great deal of information about the objects. It can help us identify the dimensions and the materials of the colliding objects [18].

Naturally, sound simulation of solid objects has attracted a great number of researchers. In this chapter we discuss the parts of their work which are relevant to our approach to sound simulation of granular materials. We also present the method we decided to use for simulation of sound caused by the interactions between granular material and surrounding solid objects.

3.1 Modal synthesis

Gaver in Articles [16] and [17] proposes a technique for synthesising sounds produced by the solid objects being hit by a mallet. The method utilises a formula in Equation 3.1, which gives the sound of a single impact.

$$G(t) = \sum_n \Phi_n e^{-\delta_n t} \cos \omega_n t \tag{3.1}$$

$G(t)$ is the waveform for the impact that is dependant on the time t. It is important to note that t is relative to the time when the impact occurred. More precisely the relation between a total value of the waveform G_{total} and the impact occurring at time t' is given in Equation 3.2.

$$G_{total}(t) = G(t - t') \tag{3.2}$$

The waveform $G(t)$ is a sum of multiple components (called partials). Each partial is controlled by three parameters Φ_n, δ_n and ω_n. Gaver [16], [17] provides the explanation of these parameters and their mapping to the perceived characteristics of the sound:

- $\boldsymbol{\Phi_n}$ - the multiplier and the initial value of the partial ($G(0) = \sum_n \Phi_n$). It controls the overall loudness of the partial. It can be mapped to the force applied in the collision (i.e. the "strength" of the contact) or the proximity of the colliding object to the listener.

- $\boldsymbol{\delta_n}$ - the damping of the partial. Value of δ_n is used in exponential term, which diminishes with increasing time. This parameter can be mapped to the material of the object. For example, wooden objects produce sounds that fade sooner than the sounds produced by metal objects.

- $\boldsymbol{\omega_n}$ - the frequency of the partial. The spacing of the partials in the frequency range maps to the size and configuration of the object (see [17]).

The values of these parameters, together with a number of partials, forms a set of values that defines the sound. We can associate such a set of values with each solid object and thus define its sound. Although Gaver doesn't use the term "**modal synthesis**" in Articles [16] and [17], this name is typically used for approaches using the formula in Equation 3.1. The term "modal synthesis" can be found, for example, in Articles [52], [14], [6]. A component in Equation 3.1 is then called "**mode**".

Van den doel [52] suggests using a matrix of initial values $A_{n,k}$. The dimensions of the matrix are $N \times K$ and its meaning is following. The surface of a solid object is sampled with K points. For k-th point, the initial values are defined as $\Phi_i = a_{i,k}$ for $i = 1 \ldots N$, where N is the number of the modes. Value of element $a_{i,k}$ is the initial value of the i-th mode when the object is hit at location of the k-th sampling point.

Concept of modal synthesis has a several advantages. First, it can be efficiently implemented in complex domain [16]. The waveform $G(t)$ is digitally represented by a collection of regularly spaced samples:

$$G(0), G(\Delta t), G(2\Delta t), \ldots, G(n\Delta t).$$

We can exploit this fact and the properties of exponential function. Namely:

$$e^{t+\Delta t} = e^t e^{\Delta t}.$$

By transforming the Equation 3.1 into complex domain, we can compute the value of the next sample efficiently by one complex multiply, instead of costly evaluation of the cosine function. This approach is often used when dealing with modal synthesis.

Second advantage is the scaling according to the available resources. We can dynamically change the number of synthesised modes [52]. This is especially important in real time synthesis. In a situation when many contacts occur simultaneously we can decrease the number of modes per contact instead of discarding the contacts.

3.2 Modal synthesis - values of parameters

Modal synthesis is a strong tool for synthesis of sounds created by vibrating solid objects. However, to produce meaningful and satisfying results it must be initialised with appropriate values of $A_{n,k}$, δ_n and ω_n. Although it is possible to set the values by trial and error approach, this process would most likely be tiresome. Gaver [16], [17] provides heuristics that can be used to determine the values according to the desired perceived characteristics of an object (e.g. size, material).

Pai et al. [38] presented a complex system for obtaining digital representation of the real world objects. The system is also capable of experimentally (i.e. hitting the object with a probe and processing the resulting sound) determining the modal parameters. The deficiency of this method is that it requires the physical presence of the object when modelling. In the next section we will see that modal analysis can provide modal parameters from purely digital description of an object.

3.3 Modal analysis

Modal analysis is a technique used to determine mechanical properties of solid objects. It has been well known in various engineering disciplines (e.g. mechanical engineering, aeronautics, etc.). It allows us to examine objects by using only their models, which is extremely important if the objects are too big to be tested experimentally or too expensive to risk their damage during the experiment.

As a relevant example, modal analysis is used to predict response of an object when an external force is applied. This can be used when ensuring stability of a structure (e.g. a bridge or other building). For more thorough review of possible application of modal analysis, see Book [19].

More recently modal analysis has been introduced to computer graphics community [39] and later it has been used for modelling of real-time deformation [46]. For the first time, the modal analysis has been applied to sound simulation by O'Brien et al. in Article [37]. Since then, modal analysis has become de facto standard method for synthesising sound of solid objects (see for example Articles [22], [42], [10], [55], [13] or [26]). In the remainder of this section we present an overview of modal analysis, as presented Article [37].

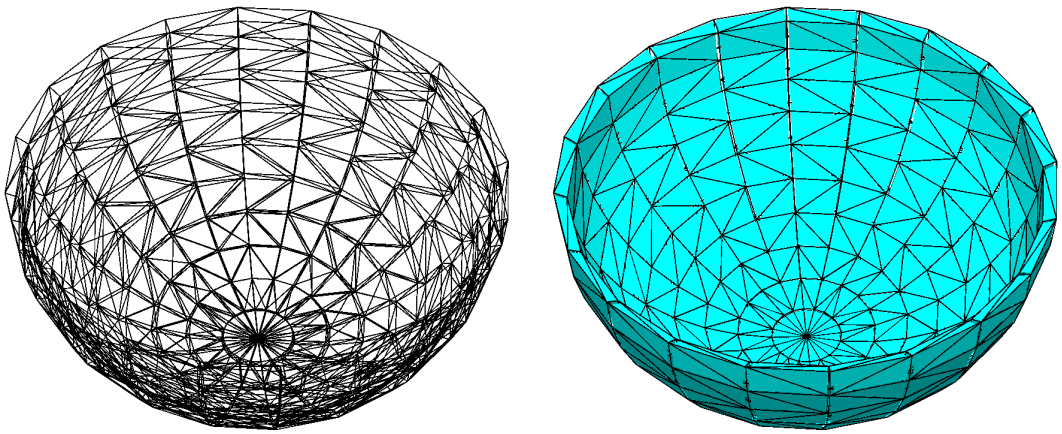

Figure 3.1: Tetrahedralization of a bowl.

Modal analysis starts by using a discrete approximation of the object in question. This may be a triangle mesh of the object's surface or a tetrahedralization of the object's volume (we will use the term "**tetrahedra mesh**"). We describe the object by Equation 3.3.

$$K(d) + C(d, \dot{d}) + M(\ddot{d}) = f \tag{3.3}$$

In Equation 3.3, d is a vector of displacements of the nodes. The nodes in this case are the vertices used in the discrete approximation, the vertices of a tetrahedra mesh. K is a nonlinear function describing the relation between nodes' displacements and the resulting internal forces. C is a nonlinear function that controls the relation between nodes' displacements and velocities and internal damping forces. M relates nodes' acceleration and nodes' momenta. f is a vector representing any external forces.

Equation 3.3 is very general, since it can contain nonlinear relations between displacement, velocities and forces. However, when considering the sound simulation, the displacements of vibrations we are dealing with, are insignificant (invisible to naked eye). Therefore, we can assume that the relations are linear and write the following equation:

$$Kd + C\dot{d} + M\ddot{d} = f. \tag{3.4}$$

Equation 3.4 defines a linear multi-degree of freedom system, where K, C and M are object's stiffness, damping and mass matrices respectively. d, $\dot{d}$ and $\ddot{d}$ are nodes' displacements, velocities and accelerations. When simulating solid objects, the matrices K, C and M are real and symmetric. K and C are positive semi-definite, while M is positive definite.

Note that Equation 3.4 is similar to Equation 3.5, which describes 1D oscillator depicted in Figure 3.2. The oscillator is composed of a mass m that is connected to a static wall using a spring with stiffness k and a damper with damping constant c. The external force applied to the mass is marked f. We find this analogy useful, as it is more probable that the reader is familiar with one dimensional oscillators, than with multi-degree of freedom systems. Interested reader may refer to Chapter 1 in Book [45] for further information about one dimensional oscillators.

$$kx + c\dot{x} + m\ddot{x} = f \tag{3.5}$$

The multi-degree of freedom system presented in Equation 3.4 provides a relationship between the external forces (e.g. contacts with other objects) and the movement of the nodes (the vibrations that produce the sound of the object). However, unless the system matrices K, C, M are diagonal, the system is coupled and therefore it is time consuming to integrate it directly. Modal analysis tries to uncouple the system by diagonalising the matrices.

Before we begin with diagonalization, let us specify some details about the damping matrix C. We use an approximation and assume that:

$$C = \alpha_1 K + \alpha_2 M. \tag{3.6}$$

This formulation of damping matrix is called Rayleigh damping and it is often used in engineering [37], [45]. Using this approximation, we can rewrite the Equation 3.4:

$$Kd + (\alpha_1 K + \alpha_2 M)\dot{d} + M\ddot{d} = f,$$

$$K(d + (\alpha_1 \dot{d}) + M(\alpha_2 \dot{d} + \ddot{d}) = f. \tag{3.7}$$

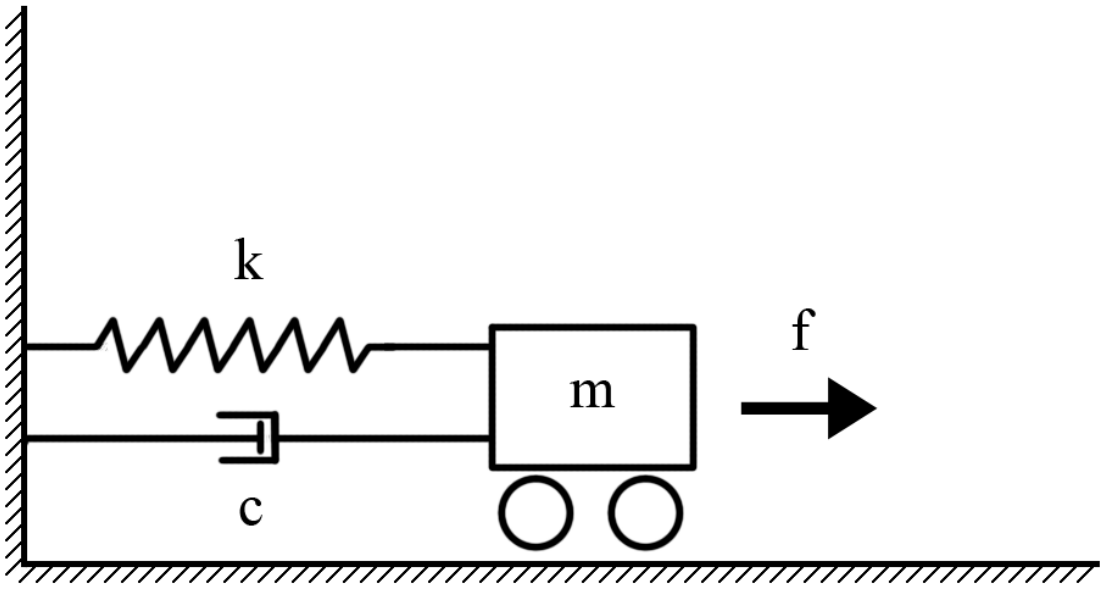

Figure 3.2: One dimensional mechanical oscillator consisting of mass m connected to a static wall using a spring with stiffness k and damper with damping constant c. The wheels underneath the mass m represent the fact that there are no friction forces between mass and the underlying surface.

M is symmetric and positive-definite, therefore we can apply Cholesky factorization to M and decompose it: $M = LL^T$. After substituting LL^T into Equation 3.7, we get

$$K(d + (\alpha_1 \dot{d}) + LL^T(\alpha_2 \dot{d} + \ddot{d}) = f.$$

We multiply the equation with L^{-1} and, to simplify, we use introduce $y = L^T d$:

$$L^{-1}K(d + \alpha_1 \dot{d}) + L^{-1}LL^T(\alpha_2 \dot{d} + \ddot{d}) = L^{-1}f,$$

$$L^{-1}KL^{-T}(y + \alpha_1 \dot{y}) + (\alpha_2 \dot{y} + \ddot{y}) = L^{-1}f. \tag{3.8}$$

Matrix $L^{-1}KL^{-T}$ is real and symmetric and it can be decomposed in the following way $L^{-1}KL^{-T} = V\Lambda V^T$, where Λ is the diagonal matrix containing eigenvalues of $L^{-1}KL^{-T}$ and the columns of orthogonal matrix V are the eigenvectors of $L^{-1}KL^{-T}$. For proof that any real and symmetric matrix can be decomposed this way, see Theorem 10.3.4 in Reference [43].

We substitute $V\Lambda V^T$ into Equation 3.8. Then we multiply the result with V^T and introduce $z = V^T y$ and $g = V^T L^{-1} f$:

$$V\Lambda V^T(y + \alpha_1 \dot{y}) + (\alpha_2 \dot{y} + \ddot{y}) = L^{-1}f,$$

$$\Lambda(z + \alpha_1 \dot{z}) + (\alpha_2 \dot{z} + \ddot{z}) = V^T L^{-1} f,$$

$$\Lambda z + (\alpha_1 \Lambda + \alpha_2 I)\dot{z} + \ddot{z}) = g. \tag{3.9}$$

In Equation 3.9, both Λ and I are diagonal. Therefore, Equation 3.9 defines system of decoupled second order differential equations. The important part is that the system is decoupled and the equations can be solved independently.

$$\lambda_i z_i + (\alpha_1 \lambda_i + \alpha_2)\dot{z}_i + \ddot{z}_i = g_i \tag{3.10}$$

Equation 3.10 gives the i-th equation from the decoupled system in Equation 3.9, where λ_i is the i-th eigenvalue. If we recall the equation of one dimensional mechanical oscillator (Equation 3.5), we see that it has the same form as Equation 3.10.

Each of the independent equations corresponds with one mode. A mode is a pattern of vibration that is defined by its frequency, damping factor and shape. The shapes of the modes are the columns of the matrix $L^{-T}V$ [37]. See Figure 3.3, for an example of a modes' shapes. The frequency and the damping factor of a mode is computed by solving Equation 3.10 for this mode.

We solve Equation 3.10 analytically to obtain solution:

$$z_i = c_{i,1} e^{t\omega_i^+} + c_{i,2} e^{t\omega_i^-}. \tag{3.11}$$

where $c_{i,1}$ and $c_{i,2}$ are arbitrary complex constants and $\omega_i^{\pm}$ is complex frequency. Complex frequency is composed from the mode's frequency (in radians) in the imaginary part and the mode's damping factor in the real part. Value of $\omega_i^{\pm}$ is computed using Equation 3.12. The values of $c_{i,1}$ and $c_{i,2}$ depend on an external force that is applied on the object (see Section 3.4).

$$\omega_i^{\pm} = \frac{-(\alpha_1 \lambda_i + \alpha_2) \pm \sqrt{(\alpha_1 \lambda_i + \alpha_2)^2 - 4\lambda_i}}{2} \tag{3.12}$$

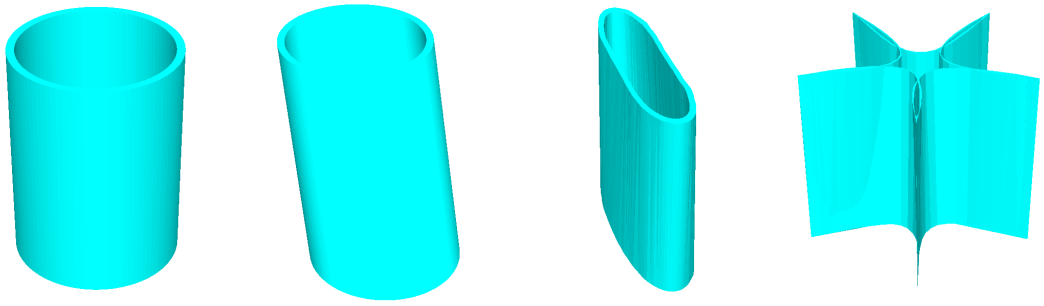

Figure 3.3: Examples of the tree different modes' shapes. The leftmost picture displays original, non-deformed model.

3.4 Applying external forces

In the analysis process described in Section 3.3, we found a set of independent oscillators (each one with its own frequency and damping) and the matrix $L^{-T}V$. Columns of this matrix are the shapes of the modes of the object. To obtain the sound of a collision, we need to apply external forces f that cause the surface vibrations and evaluate the oscillators.

According to Article [37] the forces are applied as impulses. An impulse is defined by vector f, which gives the magnitude and Δt, which gives the duration. When applying an impulse, we follow the steps from analysis and transform vector f using matrix $V^T L^{-1}$ to obtain vector $g = V^T L^{-1} f$. Vector g is then used to compute the values of constants $c_{i,1}$ and $c_{i,2}$ in Equation 3.11:

$$c_{i,1} = \frac{2\Delta t g_i}{\omega_i^+ - \omega_i^-},$$
$$c_{i,2} = \frac{2\Delta t g_i}{\omega_i^- - \omega_i^+}. \tag{3.13}$$

With the values of $c_{i,1}$ and $c_{i,2}$ defined, we may now evaluate the oscillators to obtain the resulting waveform. O'Brien et al. [37] provide a formula that is obtained after substituting Equations 3.13 and 3.12 into Equation 3.11:

$$z_i = \frac{2\Delta t g_i}{|Im(\omega_i)|} e^{tRe(\omega_i)} \sin(t|Im(\omega_i)|). \tag{3.14}$$

From Equation 3.14, we can see that the oscillator has the same basic structure as the components used in modal synthesis. The only difference is the use sine function instead of cosine. However, this change only means changing the phase of the underlying frequency function. Also, the correspondence between ω_i and the mode's frequency and damping is clearly visible. The relation between modal analysis can be seen in two ways. Modal analysis is a way to obtain object's model for modal synthesis. On the other hand, modal synthesis is reasonable model, since it corresponds to decoupled multi-degree of freedom system that describes the vibrations of an solid object.

As mentioned in Section 3.1, the values of oscillators can be effectively sampled in the complex domain. This approach advances the value of the oscillator by a sampling interval using a single complex multiplication. Thus, it doesn't need to perform the evaluation of the of cosine (or sine) function which is costly. This approach can be also applied to Equation 3.11. It is more costly, since it requires two complex multiplications and one addition. However, it still is more effective than a formula with a trigonometric function.

$$c_{i,1} e^{(t+s)\omega_i^+} + c_{i,2} e^{(t+s)\omega_i^-} = c_{i,1} e^{t\omega_i^+} e^{s\omega_i^+} + c_{i,2} e^{t\omega_i^-} e^{s\omega^- i} i \tag{3.15}$$

We summarise the efficient evaluation approach in Equation 3.15, where s is the duration of the sampling interval. It is important to note that, values $c_{i,1} e^{t\omega_i^+}$ and $c_{i,2} e^{t\omega_i^-}$ are known from previous sample and the values $e^{s\omega^{\pm} i}$ are constant during the evaluation.

Moreover, when using the Equation 3.11, applying additional external impulses is simple and straightforward. Imagine the situation that, an impact has occurred in the past. We have taken the force and computed the values of constants $c_{i,1}$ and $c_{i,2}$. We will denote these constants $c'_{i,1}$ and $c'_{i,2}$. Later, after a time t' passed, another impact occurred, resulting in new constants $c_{i,1}$ and $c_{i,2}$. The situation when we want to evaluate both impacts can be written as:

$$c'_{i,1} e^{(t'+t)\omega_i^+} + c'_{i,2} e^{(t'+t)\omega_i^-} + c_{i,1} e^{t\omega_i^+} + c_{i,2} e^{t\omega_i^-}.$$

We evaluate sum of two oscillators with different constants and one of the oscillators is advanced in time by t'. After a small reorganisation of the formula, we see that additional impulse can be modelled as a pure addition to the current value:

$$(c'_{i,1}e^{t'\omega_i^+} + c_{i,1})e^{t\omega_i^+} + (c'_{i,2}e^{t\omega_i^-} + c_{i,2})e^{t\omega_i^-}. \tag{3.16}$$

3.5 Sound rendering

By evaluating the formula from Equation 3.14 (or Equation 3.11, as the two equations provides same results), we obtain the values of z_i. When we look back at the modal analysis process, we see that values of z_i are connected to the displacements of the nodes:

$$\begin{aligned} z &= V^T L^T d \\ d &= L^{-T} V z \end{aligned} \tag{3.17}$$

When the displacements of the nodes are known, we successfully solved the first stage of the sound simulation process presented in Section 2.2. The next two stages, emission and sound propagation, can be solved for example using the approach presented in Article [22]. However, for some applications the remaining stages might be too excessive (for example due to limited computational resources). In that case, direct evaluation of the oscillators is sufficient.

Raghuvanshi and Lin [42] stated that the sound pressure is dependant on the velocity of the vibrating surface. This means that, if we are not simulating emission and sound propagation, we should be evaluating the derivative of Equation 3.11 with respect to time:

$$z_i = c_{i,1}\omega_i^+ e^{t\omega_i^+} + c_{i,2}\omega_i^- e^{t\omega_i^-} \tag{3.18}$$

3.6 Construction of system matrices

It is clear that the results of the modal analysis are dependant on the method used to model the solid objects. In other words, the method that is used to create the system matrices. There are multiple options to choose from: finite differences methods, finite element methods (see Article [37]) or a spring-mass system (see Article [42]).

The system matrices define the relationship between a pair of nodes in terms of internal forces. It is important to stress the fact that we are dealing with three dimensional objects. The dimensions are treated independently for each node. Therefore, when the object's representation has N nodes the resulting matrices have dimension $3N$.

We model the solid objects using the finite elements method used by O'Brien et al. in Article [37]. This approach had been previously presented in Article [36]. The approach uses a tetrahedralization of the object's volume. Each tetrahedron is taken as one element and for each one of them, a small stiffness and a mass matrix is produced. These matrices have dimension of 12×12, because a tetrahedron has four nodes and each dimension is treated independently. The small, 12×12 matrices define the "local" relationship between nodes within one tetrahedral element. The global system matrices are obtained by accumulating the

"local" values to the appropriate fields in the global matrices. For details see Article [36].

The properties of the object's material are used in construction of the matrices. The approach of O'Brien et al. [36] uses Lame's material parameters Λ and μ. These values can be derived from other material parameters, such as Young's modulus or Poisson's ratio[1].

For more information about a different approach, see Article [42] by Raghuvanshi and Lin. They use spring-mass system assembled from the surface of the object. This method is easily understandable and can be directly applied to 3D models of the objects, since 3D model usually contain only surface representation. Its deficiency is the fact that it models an object as a hollow mesh with given thickness. Another approach, which uses a grid approximation, is described in Article [41].

3.7 Notes

The process of modal analysis as described here exploits the fact that the damping matrix is constructed using Rayleigh damping approximation: $C = \alpha_1 K + \alpha_2 M$. However, it is possible to analyse and decouple systems with a general damping matrix (see for example Book [45]).

Although Rayleigh damping is widely used in engineering and in sound simulation, it has its deficiencies. It is clear that the values α_1 and α_2 must be carefully set, for the damping matrix to comply with the material of the object. Chadwick et al. [13] stated:"We found the popular Rayleigh damping model to be insufficient for generating realistic results in some of our examples. We extended this model with an additional damping term proportional the inverse stiffness matrix of the linear elastic system and found that the additional control provided by this model allowed us to produce much more realistic results for certain objects."

[1]Online calculator of material parameters is available at `http://www.efunda.com/formulae/solid_mechanics/mat_mechanics/calc_elastic_constants.cfm`

4. Acceleration noise

For solid objects, surface vibrations are by far the most common mechanism of producing sound waves. The way an object vibrates is affected by its shape, material and the external excitation (e.g. a collision). With previous experience, humans are able to determine some of these properties from the perceived sound. However, solid objects also produce sounds when they are subjected to a high acceleration force, typically due to a collision. Such sound is called "**acceleration noise**".

In the remainder of this thesis, when we discuss acceleration noise, we mean acceleration noise caused by collisions of solid object. We admit that if an object is rapidly accelerating due to a non-collision forces, it will produce acceleration noise. However, existence of such force is theoretical and we can restrict this discussion to the collision forces.

To illustrate the magnitude of the collision forces, we mention that Wood and Byrne [53] stated: "Although the closing velocities are relatively small, acceleration levels generated at impact can be very high, of the order $1000 - 10000 \mathrm{m\,s^{-2}}$". Richards et al. [44] report acceleration of 400g (approximately $4000 \mathrm{m\,s^{-2}}$) for the collisions of two cylinders. It is clear that generating such acceleration without a collisions is improbable.

Acceleration noise complements the sound produced by surface vibrations of solid objects. For the physically accurate simulation both must be included. On the other hand, acceleration noise is present only during the period of the collision and falls off rapidly [44]. Therefore, acceleration noise is effectively masked by the sound of surface vibrations.

Acceleration noise has been previously studied in terms of noise control (see Article [44]). Only recently has it been introduced to the sound simulation community. Chadwick et al. [13] developed a method for synthesising acceleration noise of colliding solid objects. Subsequently, the same team presented the accelerated method, in which they substitute the shape of a solid object with an ellipsoidal proxy [12].

4.1 Acceleration noise for collision of spheres

Koss and Alfredson [25] studied a case of two colliding spheres. They developed an analytical formula and compared it with experimental measurements. Experimental setup can be seen in Figure 4.1. We briefly overview their approach and present the analytical formula. Interested reader may consult the original article.

The spheres are suspended on threads. One of the two spheres is elevated and then released (this sphere is called "**impactor**"). As it drops, it gains velocity and collides with the other sphere, that is at rest (called "**impactee**"). The collision velocity is v_0 and it depends on the height from which the impactor is dropped. The close-up of the collision event, together with the position of the listener is depicted in Figure 4.2.

Koss and Alfredson [25] assume the collision is elastic (i.e. the shapes of the spheres return back to the original state, after the collision ends). They model the collision force using a Hertzian approach. Hertzian approach is common when

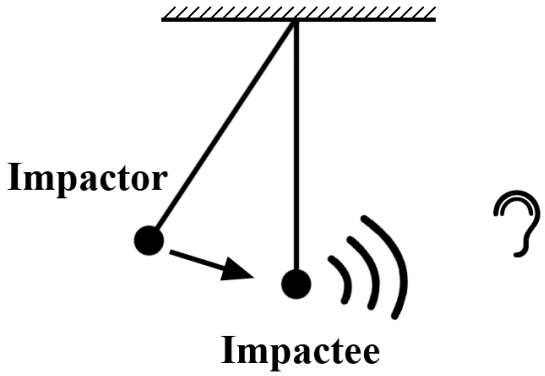

Figure 4.1: Experimental setup used to compare analytical and measured results in Article [25].

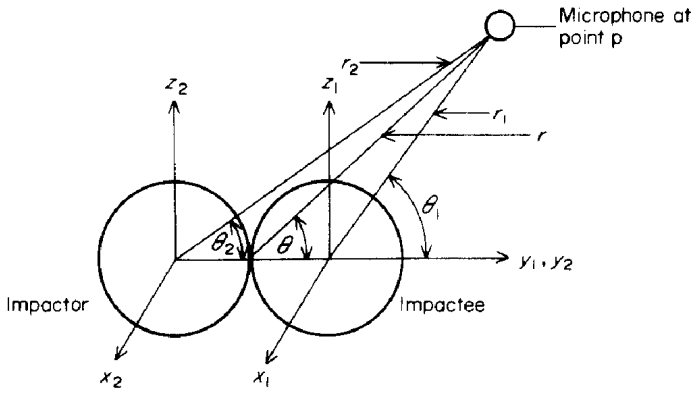

Figure 4.2: Collision of two spheres and position of the listener. Figure taken from Article [25].

modelling elastic collision forces and it has been used also by Chadwick et al. [13] in their work in sounds simulation of acceleration noise. The collision force is used to model the acceleration profile of the collision.

Formula derived by Koss and Alfredson is given in Equations 4.1 and 4.2. The formula gives the acoustic pressure of acceleration noise cause by a single sphere. The formula is separated into two distinct cases:

- For $0 < t' < d$:

$$\begin{aligned} p(r,\theta,t) = \frac{\rho_0 a_m a^3 \cos(\theta)}{4(b^4+4l^4)2r^2}\Bigg\{ &(\frac{2r}{a}-1)\Big[(8l^3b+4lb^3)\cos(bt')+ \\ &+8b^2l^2\sin(bt')\Big] - 4b^4\sin(bt') - (8l^3b+4lb^3)\cos(bt')+ \\ &+(\frac{2r}{a}-1)\Big[(4b^3l-8bl^3)\cos(lt') - (8bl^3+4b^3l)\sin(lt')\Big]e^{-lt'}+ \\ &+\Big[(4b^3l-8bl^3)\cos(l(t'-\frac{\pi}{2l})) - (8bl^3+4b^3l)\sin(l(t'-\frac{\pi}{2l}))\Big]e^{-lt'}\Bigg\}+ \\ &+\frac{\rho_0 a_m a^3\cos(\theta)}{2r^2}\sin(bt') \end{aligned} \tag{4.1}$$

- For $t' > d$

$$\begin{aligned} p(r,\theta,t) = \frac{\rho_0 a_m a^3 \cos(\theta)}{4(b^4+4l^4)2r^2}\Bigg[&(\frac{2r}{a}-1)\Bigg\{\Big[(4b^3l-8bl^3)\cos(l(t'-d))- \\ &-(8bl^3+4b^3l)\sin(l(t'-d))\Big]e^{-l(t'-d)}+ \\ &+\Big[(4b^3l-8bl^3)\cos(lt') - (8bl^3+4b^3l)\sin(lt')\Big]e^{-lt'}\Bigg\}- \\ &-\Bigg[(8bl^3-4b^3l)\cos(l(t'-d-\frac{\pi}{2l}))+ \\ &+(8bl^3+4b^3l)\sin(l(t'-d-\frac{\pi}{2l}))\Bigg]e^{-l(t'-d)}- \\ &-\Bigg[(8bl^3+4b^3l)\sin(l(t'-d-\frac{\pi}{2l}))\Bigg]e^{-lt'}\Bigg] \end{aligned} \tag{4.2}$$

where

- a - radius of the colliding spheres.
- E - Young's modulus of the spheres' material.
- ν - Poission's ratio of the spheres' material.
- d - duration of the collisions. Koss and Alfredson [25] used experimentally measured collision duration. However, a formula can be found in Article [29].
- $b = \frac{\pi}{d}$
- a_m - maximal acceleration of the spheres due to the collision force.
- ρ_0 - density of the surrounding medium (i.e. the air).
- $l = \frac{c}{a}$ - where c is the speed of sound.

- r - the distance between sphere's centre and the listener's position.
- θ - angle between collision normal and the direction towards the listener.
- t - time.
- $t' = t - \frac{r-a}{c}$ - time accounted for delay caused by the distance between sphere's surface and the listener.

The formula predicts acceleration noise of a single sphere. In the studied scenario both spheres are subjected to acceleration in the opposite directions. Therefore, to obtain correct value of acoustic pressure, the formula must be evaluated twice with different values of r and θ and the results are added together (with opposite signs).

The resulting pressure is depicted in Figure 4.3. Impactee is closer to the listener, therefore the sound wave arrives sooner than the wave from impactor. Note the opposite pressure signs, as the spheres are accelerated in the opposite directions.

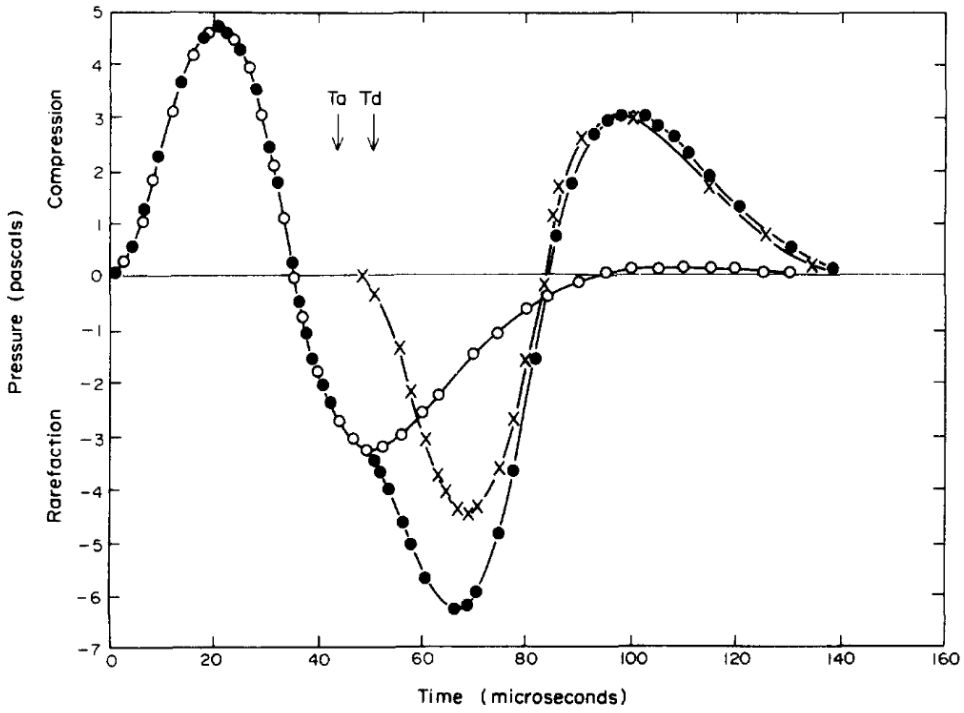

Figure 4.3: Results of the analytical formula for acceleration noise of colliding spheres (Equations 4.1 and 4.2). ○ - pressure from impactee; × - pressure from impactor; ● - total pressure; Figure taken from Article [25].

5. Sound of granular materials

In this chapter we introduce our method for sound simulation of granular materials. We propose an approach that models the sound produced by the collisions of the particles of granular material using an acceleration noise. Instead of the real shapes of the particles, we use spherical proxy shapes. Sound produced by each collision is modelled as an acceleration noise produced by two colliding spheres. We also present a probabilistic approach to generation of the collisions of the particles of granular material.

5.1 Sound producing mechanism

When a granular material is in movement (for example, sugar being poured into a bowl), it produces a typical sound. From observation it is clear that the sound we hear is a combination of two distinct sound producing mechanisms:

- **Granular collisions** - the collisions among the particles of the granular material itself.
- **Solid objects collisions** - the collisions between the particles of the granular material and the surrounding solid objects.

The second mechanism is very important for multiple reasons. First it produces sound that is much louder than the one produced by granular collisions only. This fact is immediately seen, when we compare Recordings 28 and 29. These are the recordings of the same material being poured into a metal cup. In the case of Recording 28 , the metal cup is empty. Whereas in the case of Recording 29, the metal cup has been filled with a small amount of material.

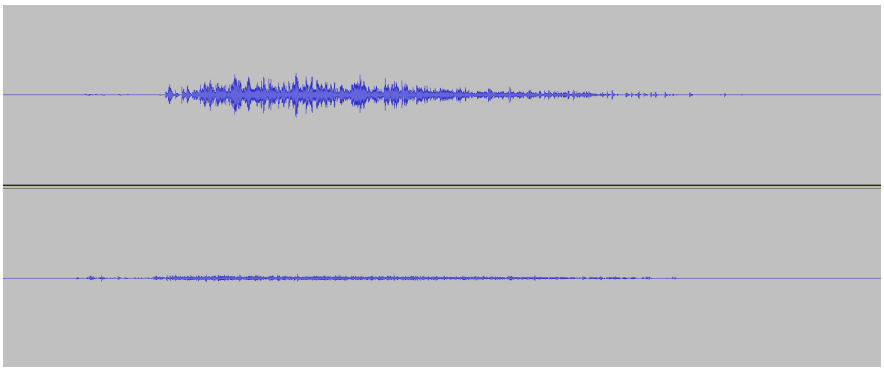

Figure 5.1: Waveforms of plastic disc-shaped granular material poured into a ceramic cup. Comparison of empty cup (top picutre) and a cup filled with granular material (bottom picture).

The main difference between the two recordings is that, in the case of an empty cup, the falling particles collide with the cup itself. In the second case the falling particles collide with the particles already present in the cup. They might

get rebounded into the cup's walls. However, the overall number of collisions between the particles and the metal cup is much smaller than in the first case.

In real world we rarely hear the sound of granular collisions only. The situations usually include the contacts with solid objects and we, as humans, find this sounds natural. Moreover, the sound from solid objects collisions reveal a great deal of information about the solid object: material, size. Therefore, we conclude that sound simulation of granular materials must involve simulation of both mechanisms: granular collisions and solid objects collisions.

5.2 Sound of solid objects collisions

When a solid object is hit by the particles of a granular material, its surface vibrates and thus produces sound. Sounds produced by surface vibrations of solid objects have been studied by many researchers (see Section 1.4 for a brief overview). Therefore, we can use their work when modelling sounds caused by the particles of a granular material colliding with a solid object.

We use modal analysis approach that is presented in Chapter 3. Using this approach we can obtain sound model of virtually any solid object. The model is then used with appropriate external forces resulting from collisions between the particles and the solid object.

5.3 Sound of granular collisions

When the particles of a granular material collide, they produce sound. Chadwick et al. [13] claim that surface vibrations of small objects (such as ball bearings or dice) occur at frequencies above the audible range. This description also fits the particles of granular materials we are interested in. Their size is in order of millimetres. Therefore we hypothesise that, the sound for granular collisions is an acceleration noise, and thus it can be modelled as acceleration noise.

To support this hypothesis, we conducted simple experiment. We applied modal analysis to the models of spherical particles with different radii. The particles were approximated by a tetrahedra mesh with 42 nodes. The tetrahedra mesh is depicted in Figure 5.2. The material data used in the analysis are: density $\rho = 1602\text{kg}\,\text{m}^{-3}$, Young's modulus $E = 20\text{MPa}$ and Poisson's ratio $\nu = 0.35$.

The resulting spectra of surface vibrations are depicted in Figure 5.3. From the top to the bottom of the figure, the radius of the particle is 0.01m, 0.005m, 0.001m, 0.0005m respectively. It is clear that, with smaller particles the vibration frequencies are higher and outside the audible range. Therefore, we assume that modelling the sound of granular collisions with the acceleration noise is sufficient.

Chadwick et al. in Article [12] present a method for fast simulation of acceleration noise. The method takes advantage of ellipsoidal proxies, which are used instead of the original objects. Chadwick et al. state that, their approach is effective for scenarios involving large numbers of small objects (e.g. debris from fracture simulation). The particles of granular materials precisely suits this description. Therefore, we follow the approach of Chadwick et al. and use approximation objects to model acceleration noise of granular collisions.

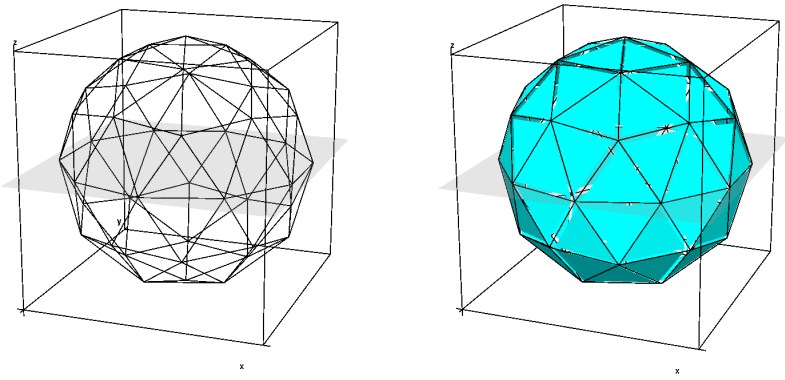

Figure 5.2: Tetrahedra mesh that approximates a spherical particle is used in modal analysis to determine vibrational frequencies of the particle.

The difference between our approach and the one presented in Article [12] is the used proxy objects. We use spherical instead of ellipsoidal shapes. The main advantage is that, the acceleration noise of colliding spheres can be obtained in closed form formula (see Chapter 4.) On the contrary, the method of Chadwick et al. requires a precomputed soundbank. We assume that using spherical instead of ellipsoidal proxies is tolerable, since the approximated particles are small. Moreover, the ellipsoidal proxies are approximation to and not the real object in the first place.

In Chapter 4 we presented the formula for acceleration noise of colliding spheres (originally developed by Koss and Alfredson in Article [25]). The formula is given in Equations 4.1 and 4.2. The formula is dependant on many different variables and material constants. However, we can pose certain limits.

- Surrounding medium - we can assume that the surrounding medium is fixed during the period when granular collision occur. Therefore the values of medium density ρ_0 and speed of sound c are constant.
- Granular material - we consider only scenarios involving single type of granular material. As a result, the values of Young's modulus E, Poisson's ratio ν and the radius of the spherical proxy shapes a are constant.
- Listener - the position of the listener is constant during the simulation.

Considering these limits, we are left with the formula that is controlled by four parameters:

- t - time when the impact occurred,
- $\vec{x}$ - location of the impact,
- $\vec{n}$ - normal of the impact,
- v_0 - velocity of the impact.

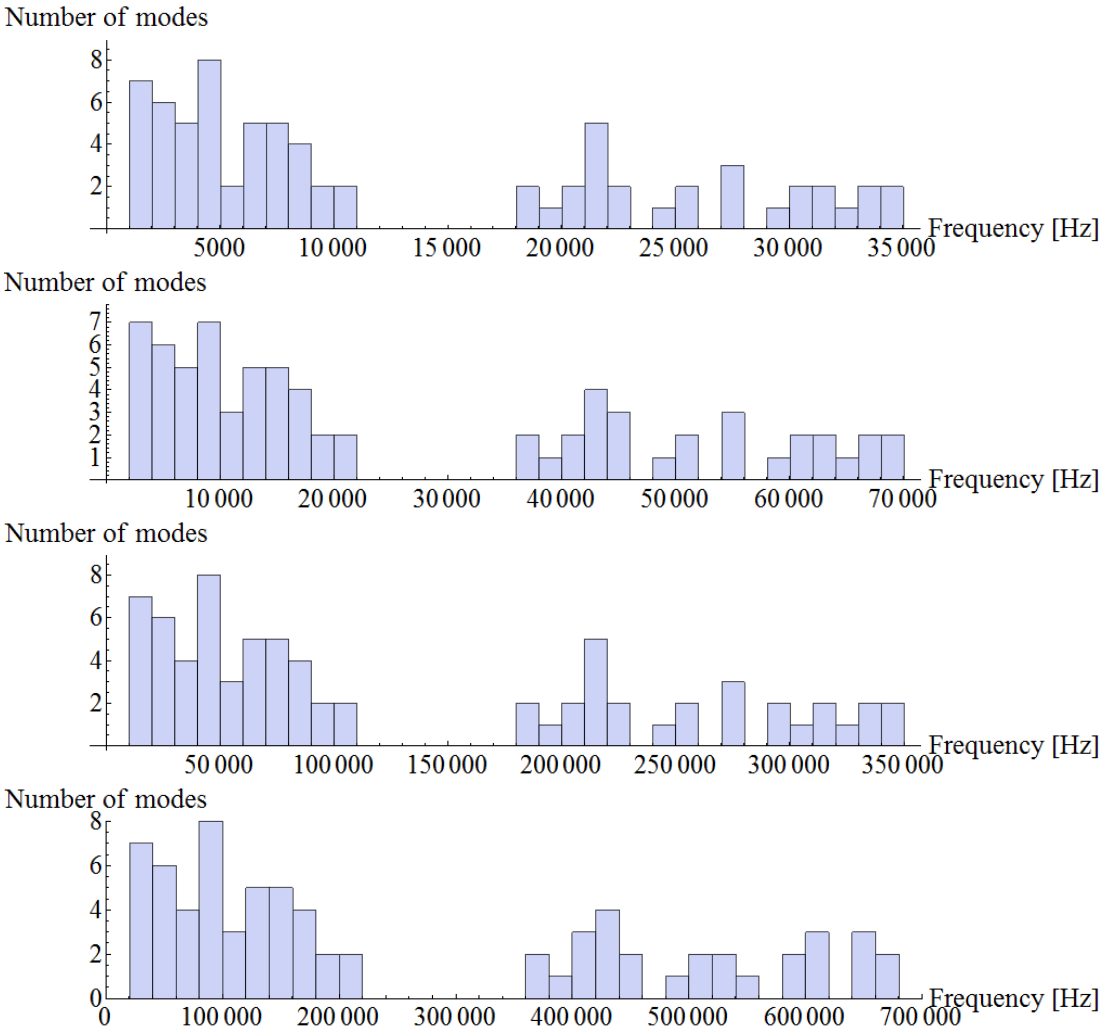

Figure 5.3: Spectra of the surface vibrations of the spherical particles with different radii. From top to the bottom, the radius is 0.01m, 0.005m, 0.001m, 0.0005m respectively.

Note that location $\vec{x}$ and normal $\vec{n}$ are used to determine the values of r and θ used in Equations 4.1 and 4.2. As mentioned in Chapter 4, each granular collision involves two particles. Therefore, for each granular collision we evaluate the formula twice with different values of r and θ.

5.4 Importance of collision parameters

In Section 5.3 we showed that each granular collision is defined by four parameters: time t, location $\vec{x}$, normal direction $\vec{n}$ and velocity v_0. Now we discuss the relative importance of these parameters in relationship to the resulting sound. We use the following experimental approach. We used the Dynamo[1] event driven simulator to simulate a scenario involving a granular material. From the simulation, we extracted the information about all collisions between the granular particles. We

[1] `http://dynamomd.org/`

randomly changed the properties of each collision and simulate the sound using the method presented in Section 5.3. We then compared the difference between the sound of the original and the randomly modified collisions.

It is clear that larger changes would cause more significant differences. We limit ourselves to only small changes. First, we test the influence of the location. We split the simulation space using a regular grid. For each collision, the new location is uniformly sampled from the cell the collision originally belonged to. The results can be seen in Figure 5.4. There isn't much difference between the original collision data (the top picture in Figure 5.4) and the collisions with random location, generated within 1cm cells (the middle picture). The difference become more significant when we increase the size of the grid cells to 2cm.

Changing the location of a collisions affects the distance r and the angle θ to the listener. Thus, it influences the overall loudness (Equations 4.1 and 4.2 contain "$\cos(\theta)$" term) and the time, when the sound arrives to the listener. However, we conclude that changing the location within a grid cell has small impact on the resulting sound.

In contrast to the random locations, influence of random normals is very strong. The comparison between the original collisions and the collisions with random normal is depicted in Figure 5.5. The sound of the original collisions is louder than the sound produce by the collisions with random normals.

Changing the normal of a collision changes the angle to the listener θ. Consequently, it affects the overall loudness of the produced sound (recall the "$\cos(\theta)$" term in Equations 4.1 and 4.2). The loudness of a collision is also affected by its velocity: the higher the velocity, the louder the sound (see Table 6.1). We hypothesise that the particular combination of high velocity collisions with normal direction pointing towards listener contributes greatly to the sound.

To support our hypothesis, we modified the collision data in the following way. We generated random normal direction for the collisions with $v_0 < v_{limit}$. For the collisions with $v_0 >= v_{limit}$, we use the original normal direction. Comparison of the original collision data and the random normal direction with velocity limit is showed in Figure 5.6. When using the velocity limit, the difference between the original collisions and the randomised data is less significant than without the limit. Note that when using $v_{limit} = 0.5\mathrm{m\,s^{-1}}$, 96.42% of the collisions were assigned the random normal. This case is depicted in the middle picture of Figure 5.6. The bottom picture of Figure 5.6 shows the result with velocity limit $v_{limit} = 1.0\mathrm{m\,s^{-1}}$. With this value, 99.33% of the collisions were assigned the random normal. We conclude that, from the viewpoint of the resulting sound, there is a correlation between the collisions' normal directions and velocities.

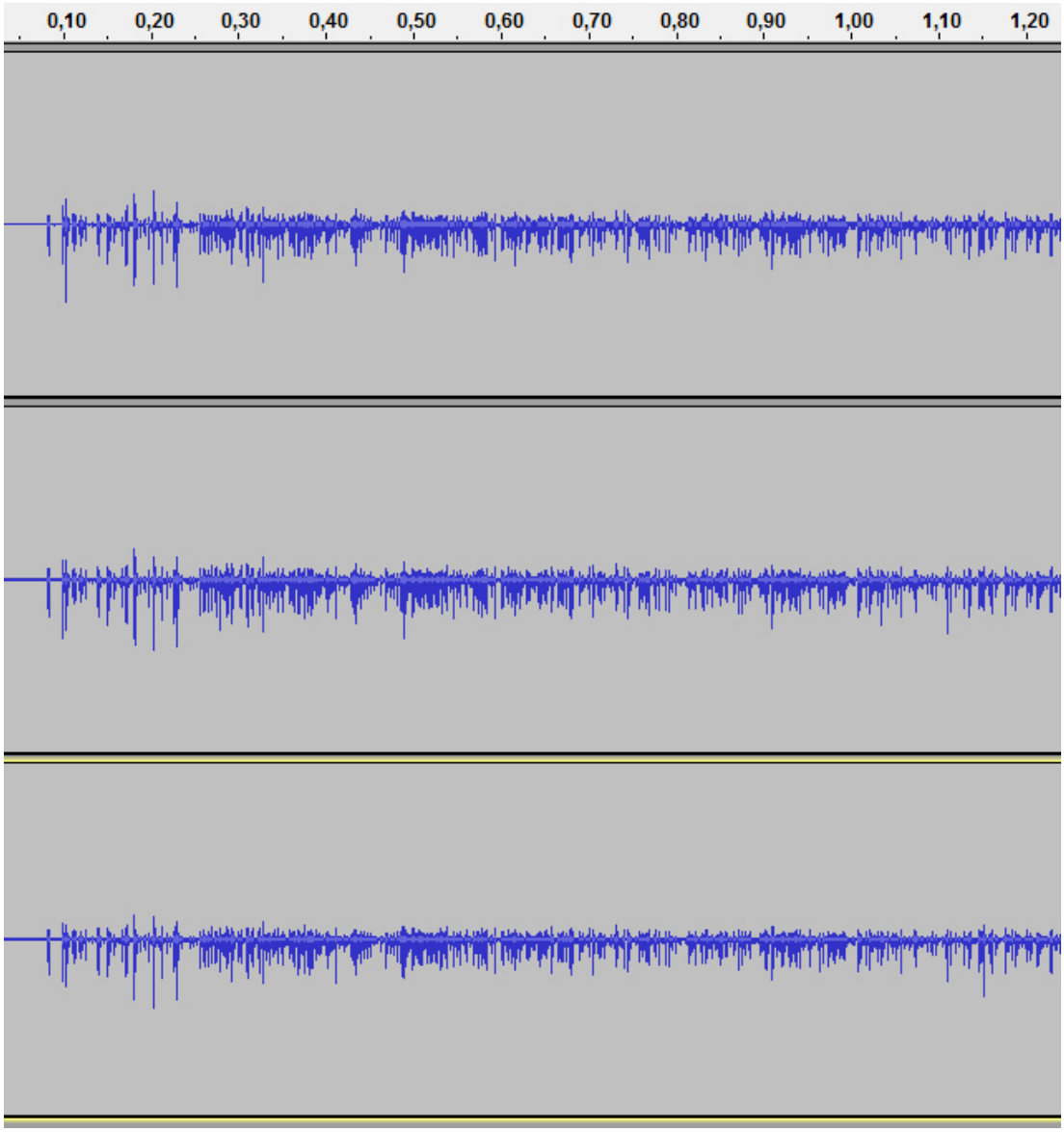

Figure 5.4: Comparison of the waveforms with randomised locations of the granular collisions. The top picture shows the waveform of Sound sample 73 produced by the original collision data. The middle picture shows the waveform of Sound sample 74 produce by the collisions with locations randomly generated within 1cm grid cells. The bottom picture (waveform of Sound sample 75) was created by the collisions with random locations within 2cm grid cells.

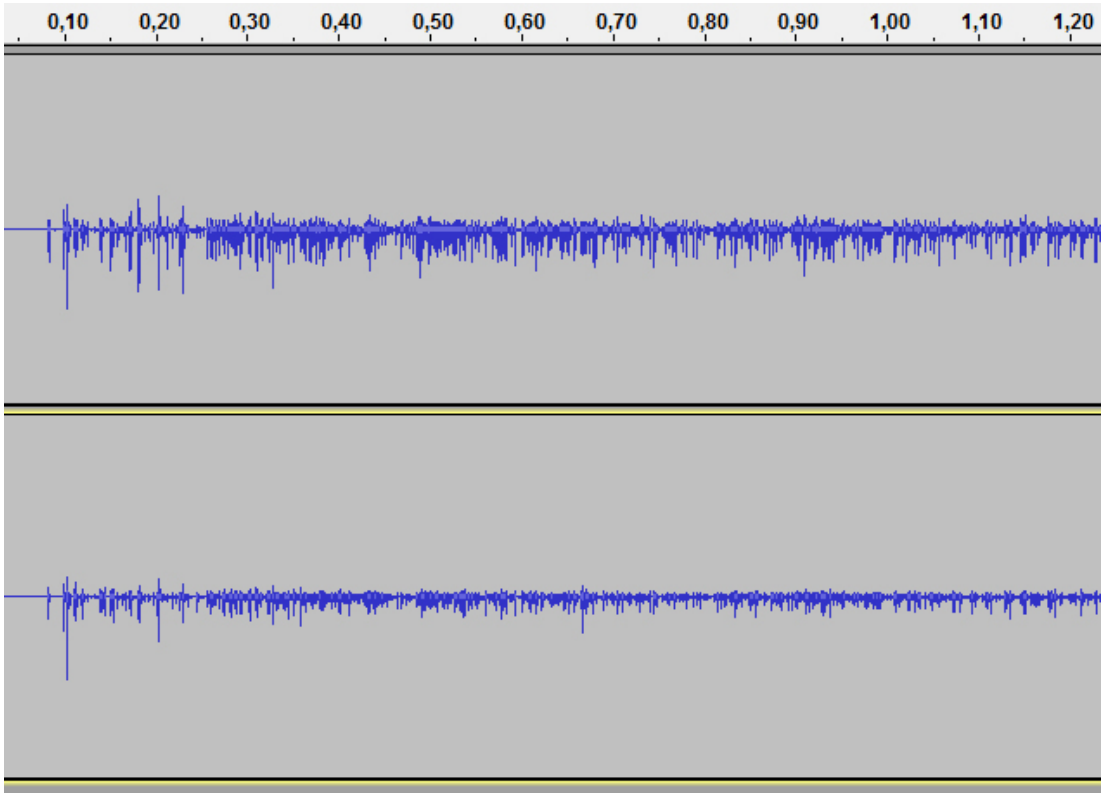

Figure 5.5: Comparison between waveform of the original collisions from Sound sample 73 and the collisions with random normals from (Sound sample 76).

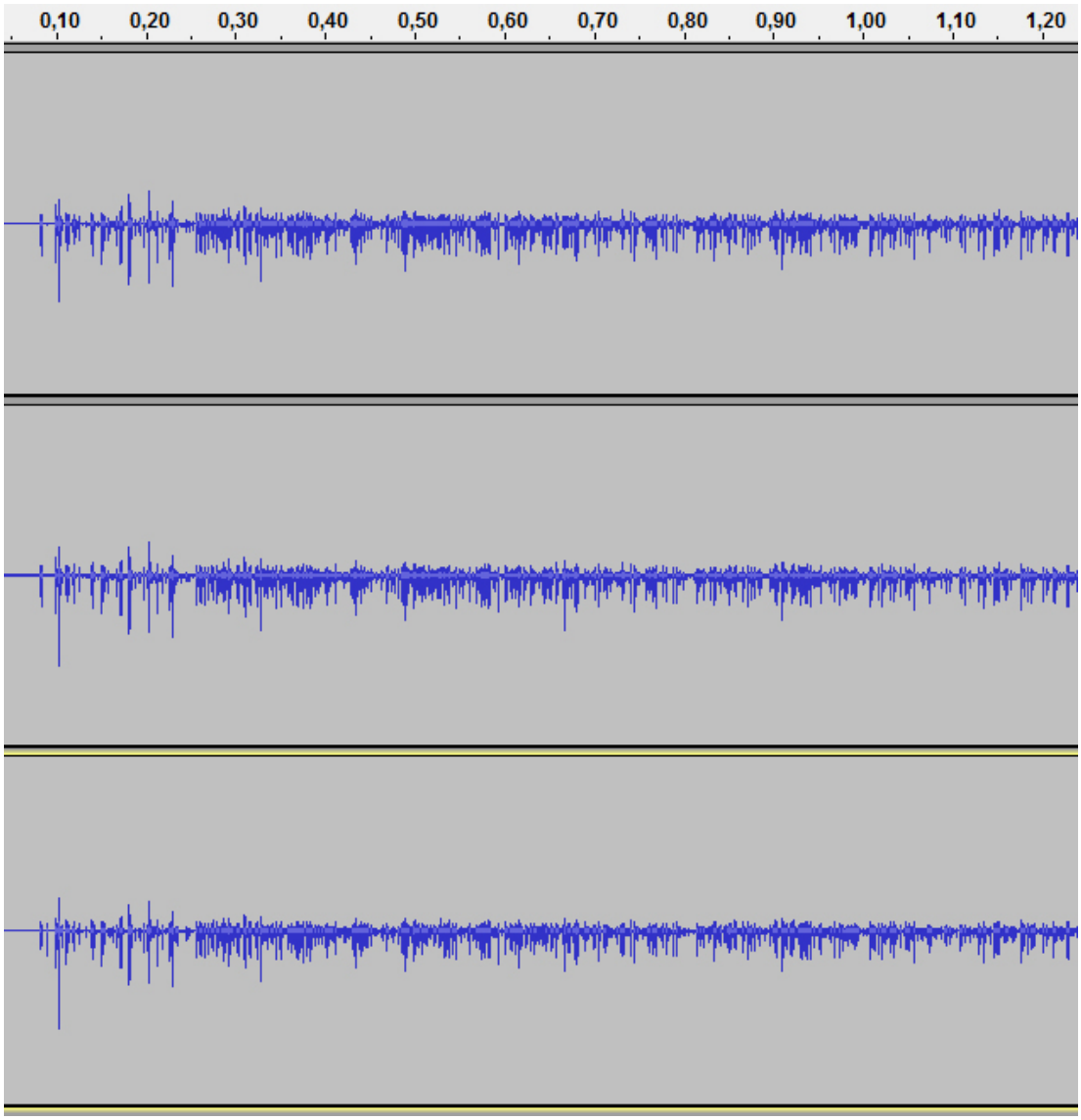

Figure 5.6: Comparison between waveform of the original collisions and the random normals for the collision within velocity limit. Top picture shows the waveform of the original collisions from Sound sample 73. The middle picture shows the waveform of collision with random normals from Sound sample 79, where random normals were assigned only to the collisions with $v_0 < 0.5\mathrm{m\,s^{-1}}$. In the bottom picture from Sound sample 80, the velocity limit is set to $1.0\mathrm{m\,s^{-1}}$.

5.5 Granular collisions - probabilistic approach

In Section 5.3 we presented our approach towards modelling the sound of granular collisions. We use an analytical formula to obtain acceleration noise of the granular collisions. The formula can be applied to the collision data, i.e. the collection of all granular collision that occur during the simulation.

However, most of the methods for animation or simulation of granular materials don't provide sufficient information about the granular collisions (for brief overview of these methods, see Section 2.4). Methods using the discrete approach may miss some of the collisions, whereas in the continuum approach the collisions are not even considered. To overcome this deficiency we investigate a probabilistic approach to collision data generation.

Each contact is defined by its four properties: time of occurrence t, location $\vec{x}$, normal direction $\vec{n}$ and velocity v_0. We define

$$p_g(t, \vec{x}, \vec{n}, v_0) \tag{5.1}$$

to be the probability density that an impact occurs at the time t and the location $\vec{x}$ and it has the normal direction $\vec{n}$ and the velocity v_0. If the value of p_g is known, it can be sampled to obtain the collision data.

Considering all different scenarios for the simulation of granular material, it is highly unlikely that we can find p_g as a closed form expression. Take two examples, both take 20 seconds. In one of them, sugar is continuously poured into a bowl. In the other, a spoon is dropped into a bowl of sugar, the spoon is left there for 15 second and then is taken out again. In the first case, the granular collisions occur during the whole duration of the simulation and their properties are stable during the simulation (i.e. the sugar is poured in the same way in the first second, as it is in the last second of the simulation). On the other hand, in the second case, there is a long period when no collision occur. Moreover, the collisions caused by the drop of the spoon and by the extraction, might have different properties.

We believe that finding global probability density function p_g would be difficult. Instead we propose a localised approach. The duration of the simulation is split into regular temporal windows and the space of the simulation is split into spatial cells using a regular grid. We use the term "**window/cell**" when speaking about events occurring inside a given spatial cell, during a given temporal window. We denote the local PDF for the window w (it is the time interval $[t_w,\ t_{w+1}]$) and the spatial cell c as:

$$p_{w,c}(t, \vec{x}, \vec{n}, v_0) \tag{5.2}$$

Local PDF for each window/cell is in fact a marginal PDF. Therefore its relationship with the global collision PDF p_g is:

$$p_{w,c}(t, \vec{x}, \vec{n}, v_0) = \begin{cases} \dfrac{p_g(t, \vec{x}, \vec{n}, v_0)}{const_{w,c}} & \text{if } t \in w \wedge \vec{x} \in c \\ 0 & otherwise \end{cases} \tag{5.3}$$

where the normalization constant $const_{w,c}$ is defined as:

$$const_{w,c} = \int_{t_w}^{t_{w+1}} \int_{vol(c)} p_g(t, \vec{x}, \vec{n}, v_0) \mathrm{d}\vec{x}\mathrm{d}t \tag{5.4}$$

We assume that the local PDFs $p_{w,c}$ and the values of normalization constants $const_{w,c}$ are known. To generate a sample from p_g we first choose the window/cell according to the values of $const_{w,c}$ and then we sample the corresponding $p_{w,c}$ for a collision. The values of $p_{w,c}$ and $const_{w,c}$ are expected to be corresponding to the visual simulation of the granular material. In Section 5.6 we present the reconstruction of local PDFs from an event driven simulation.

5.6 Probabilistic approach - details discussion

To verify the probabilistic approach presented in Section 5.5, we need to find probability density functions in the window/cells. We use the collision data from the Dynamo simulations to approximate $p_{w,c}$.

To reconstruct the local probability density functions $p_{w,c,}$, we first split the granular collisions into corresponding window/cells. More precisely, the pair of window w and cell c gets the impacts with:

$$t \in [t_w,\ t_{w+1}) \wedge \vec{x} \in \mathrm{Vol}(c).$$

From these impacts we reconstruct the local PDF $p_{w,c}$. We choose the simple histogram reconstruction method.

However, first we must discuss the domain of $p_{w,c}$. If we use the naive approach, we are left with 7-dimensional space as the domain of $p_{w,c}$. t and v_0 are scalars, $\vec{x}$ is three dimensional vector and $\vec{n}$ can be expressed in spherical coordinates using two values. We use the fact presented in Section 5.4 that the small changes of the collisions' locations have only small influence on the resulting sound.

We will consider $\vec{x}$ to be independent from t, v_0 and $\vec{n}$ and formulate $p_{w,c}$ as:

$$p_{w,c}(t, \vec{x}, \vec{n}, v_0) = p_{w,c}(\vec{x}) \cdot p_{w,c}(t, \vec{n}, v_0). \tag{5.5}$$

As a result, we won't reconstruct $p_{w,c}(t, \vec{x}, \vec{n}, v_0)$, but only the 4-dimensional $p_{w,c}(t, \vec{n}, v_0)$. We approximate $p_{w,c}(\vec{x})$ by the uniform distribution within the volume of cell c. We argue that, with cells being small enough the error of approximation is tolerable (see comparisons in Section 5.4).

If we use the approach presented in Section 5.5 directly, we need to reconstruct values of normalisation constants $const_{w,c}$. According to Equation 5.3, constants $const_{w,c}$ relate the local density functions $p_{w,c}$ to the global PDF p_g. Recall the definition of $const_{w,c}$ from Equation 5.4:

$$const_{w,c} = \int_{t_w}^{t_{w+1}} \int_{vol(c)} p_g(t, \vec{x}, \vec{n}, v_0) \mathrm{d}\vec{x}\mathrm{d}t.$$

We see that, the $const_{w,c}$ is equal to probability that a collision occur during time window w and inside the volume of cell c. Therefore, we can approximate the value of $const_{w,c}$ as:

$$\frac{\#\text{ collisions within window/cell w,c}}{\#\text{ all collisions}}.$$

However, we use different approach. The meaning of $const_{w,c}$ is that it controls how many collisions will be sampled from $p_{w,c}$. As such, we don't need to know

the value of $const_{w,c}$, but we need to determine the number of samples for $p_{w,c}$. One option is to use the exact number of collisions, from which we reconstruct the local PDFs, that belong to the window/cell w, c. Another option is the use of Poisson distribution. Cook in Article [14] states that, the time distribution of collisions of granular material in maracas resembles Poisson process. Number of events in Poisson process is controlled by Poisson distribution. We use the same fact and assume that the number of collisions generated for each cell can be approximated by the Poisson distribution. The number of collisions belonging to the window/cell w, c is used as the λ parameter of the distribution (which is equal to the expected value for the Poisson distribution). Therefore, we define the number of samples from $p_{w,c}$ as:

$$\#\text{ samples from } p_{w,c} \sim Pois(\#\text{ collisions belonging to window/cell } w, c). \quad (5.6)$$

The naive use of approach presented in Section 5.5 has one deficiency. It requires that the PDFs $p_{w,c}$ are known for all window/cells during the whole sampling process. Therefore, we modify the sampling procedure. We iterate through the window/cells and for each one we reconstruct the local PDF $p_{w,c}$. We use above-mentioned method to determine the number of collisions that we need to sample for this window/cell and sample them. The random collisions are added to the global list of sampled collisions. When the sampling is done for all window/cells, we sort the global list according to the time of occurrence.

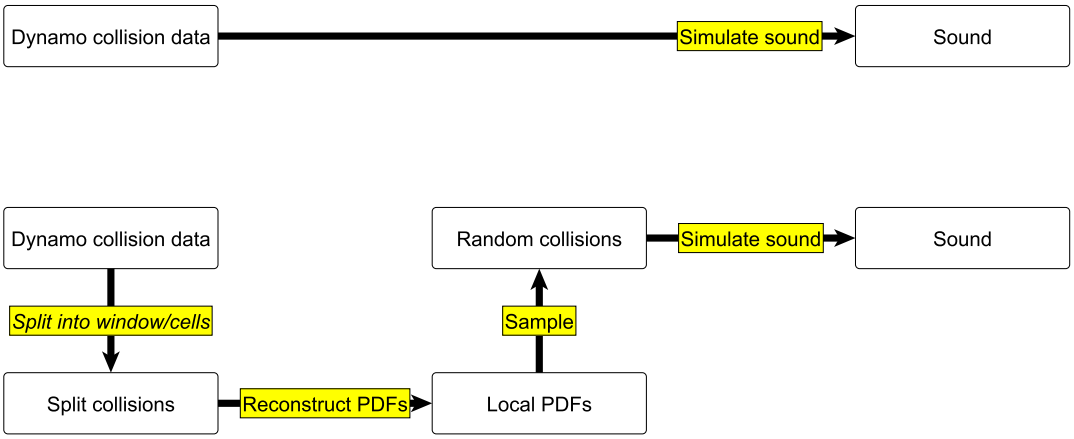

Figure 5.7: The workflow of the probabilistic approach that uses local PDFs reconstructed from the collision data from the Dynamo simulation. The top picture shows the situation when the sound is synthesised directly from the Dynamo collision data. The bottom picture shows the workflow presented in Section 5.6.

6. Results

In this chapter we present the results obtained from our method for sound simulation of granular material. In Section 6.1 we present results from verification of our approach that uses acceleration noise to model the sound of granular collisions. Then, in Section 6.2, we present an application of probabilistic approach, which is described in Section 5.5.

6.1 Results - direct collision data

First, we verified the viability of our approach of using acceleration noise to model the sound of granular collisions. To obtain granular collision data, we used the Dynamo[1] event driven simulator. We chose Dynamo because it is open source, effective yet relatively simple project. We modified the source code to obtain necessary data about all collisions that occur during the simulation. The advantage of the event driven simulation is that it doesn't miss collisions as the time-stepped simulations do.

Once the granular collision data are available, we filter them to reduce the number of collisions, for which we need to generate acceleration noise. We evaluated the formula in Equations 4.1 and 4.2 with different values of collision velocity v_0. The results are summarised in Table 6.1. According to Book [8], audible threshold is $2 \cdot 10^{-5}$Pa. We determined that the collisions with velocity $v_0 < 0.0001\mathrm{m\,s^{-1}}$ can be removed. We guess that even more radical filtering can be applied. However, it may result in loosing important collision information.

With the collision data available, we can use the method presented in Section 5.3. We generate acceleration noise for each collision and sum them together into the resulting waveform. The results are listed in Table 6.2. We compare the simulation results with the recordings of a similar experimental scenario. The scenario is designed to exclude all sound that is not produced by the granular collisions. For details about the experimental scenario, see Appendix B.

The sounds from the simulations for the different granular materials exhibit the differences between the materials. These differences resemble the inter-material differences captured by the recordings. Admittedly, there are discrepancies between the simulated sounds and the corresponding recorded sounds of the same material. The discrepancies are in part caused by the fact that our sound simulation workflow omits the sound wave propagation step and by the limited amount of the granular material which is present in the simulation. Although the scenarios in the simulations are similar to the real world experiments, there are some differences (see Section B.2 in Appendix B) which also accounts for the difference between the simulated sounds and the recordings. We must also stress that, recording the sound of only granular collisions is extremely problematic. Nevertheless, the simulated sounds capture the main characteristics of the simulated scenarios and provide believable sound of granular materials.

In the Dynamo simulations, we approximated the solid objects by a collection of static particles (see Appendix B). The static particles are treated in the same

[1] Dynamo website can be found at `http://dynamomd.org/`.

way as the particles of granular material. As a result, we are able to extract the information about collisions between particles of the granular materials and the static particles, i.e. the solid body collisions. We use the method presented in Chapter 3 and model the external forces that are applied on the solid object according to the solid object collision data.

Table 6.1: Values of maximal acoustic pressure for acceleration noise depending on the collision velocity. The result were obtained using a material with $\rho = 2520\text{kg}\,\text{m}^{-3}$, $E = 72\text{GPA}$, $\nu = 0.22$ and with sphere radius $a = 0.001\text{m}$. The listener position has been set to be at $r = 0.15\text{m}$ and $\theta = 0$.

$\boldsymbol{v_0}$ [$\text{m}\,\text{s}^{-1}$]	**Max pressure** [Pa]
10^{-5}	$1.913 \cdot 10^{-7}$
$6.2105 \cdot 10^{-5}$	$2.3763 \cdot 10^{-6}$
0.0001142	$5.5211 \cdot 10^{-6}$
0.0001663	$9.24631 \cdot 10^{-6}$
0.0002184	$1.33821 \cdot 10^{-5}$
0.0002705	$1.81913 \cdot 10^{-5}$
0.0003226	$2.32380 \cdot 10^{-5}$
0.0003747	$2.84454 \cdot 10^{-5}$
0.0004268	$3.36448 \cdot 10^{-5}$
0.0004789	$3.99788 \cdot 10^{-5}$
0.0005311	$4.58131 \cdot 10^{-5}$
0.0005832	$5.23089 \cdot 10^{-5}$
0.0006353	$5.84084 \cdot 10^{-5}$
0.0006874	$6.58677 \cdot 10^{-5}$
0.0007395	$7.14722 \cdot 10^{-5}$
0.0007916	$7.93963 \cdot 10^{-5}$
0.0008437	$8.72381 \cdot 10^{-5}$
0.0008958	$9.34642 \cdot 10^{-5}$
0.0009479	0.00010
0.001	0.000109960

The sounds of solid object collisions are listed in Table 6.3. Table 6.4 then contains sounds mixed from both the granular collisions and solid objects collisions. When compared with the recordings (also present in Table 6.4), the simulated sounds are convincing. The characteristics of the granular material and the material of the solid body object are preserved in the sound. The discrepancies are once again caused by the differences between the simulated scenario and the real world experiment and by the values of the material constants for the solid objects.

Table 6.2: Comparison between simulated and recorded sounds of granular collisions. For details about the recording process and description of both the recorded and simulated scenarios, see Appendix B.

Granular material	**Rec/Sim**	**Sound sample**
Glass spheres with 2mm diameter	Simulation	Sound sample 48
	Recording	Sound sample 20
Glass spheres with 1mm diameter	Simulation	Sound sample 43
	Recording	Sound sample 13
Plastic discs with 4mm diameter	Simulation	Sound sample 53
	Recording	Sound sample 34

Table 6.3: Results from the sound simulation of solid object collisions.

Granular material	**Solid material**	**Sound sample**
Glass spheres with 2mm diameter	Ceramic	Sound sample 49
	Metal	Sound sample 50
Glass spheres with 1mm diameter	Ceramic	Sound sample 44
	Metal	Sound sample 45
Plastic discs with 4mm diameter	Ceramic	Sound sample 54
	Metal	Sound sample 55

Table 6.4: Comparison between simulated and recorded sounds of both the granular collisions and the solid objects collisions.

Scenario	**Rec/Sim**	**Sound sample**
Glass spheres with 2mm diameter and ceramic cup	Simulation	Sound sample 51
	Recording	Sound sample 15
	Simulation	Sound sample 52
	Recording	Sound sample 17
Glass spheres with 1mm diameter and ceramic cup	Simulation	Sound sample 46
	Recording	Sound sample 8
	Simulation	Sound sample 47
	Recording	Sound sample 10
Plastic discs with 4mm diameter and ceramic cup	Simulation	Sound sample 56
	Recording	Sound sample 29
	Simulation	Sound sample 57
	Recording	Sound sample 31

6.2 Probabilistic approach - results

We applied the probabilistic approach to the collision data from the Dynamo simulation. The collisions are analysed in order to reconstruct local PDFs $p_{w,c}$. The local PDFs $p_{w,c}$ are then sampled to generate the random collision data. Once the data are available, they can be treated in the same way as the original data from Dynamo simulation.

Table 6.5 contains the results for random granular collisions. When we compare the sound of random collisions obtained from our probabilistic approach with the sound of the collision data from Dynamo simulation, they are very similar. Although the random collisions sounds do miss some of the detail features, the overall properties of the sounds are preserved. Moreover, compared to the recordings of the real world experiments, the probabilistic approach produces believable results. It seems to be a viable way for the sound simulation of granular materials.

Note that the probabilistic approach can be used for the solid object collisions as well. We applied the method to the collision data from Dynamo simulations. The results are presented in Table 6.6. The comparison of mixed sounds can be found in Table 6.7.

Table 6.5: Randomly generated granular collisions. Comparison between simulation of collisions from Dynamo, random collisions and recorded sounds of granular collisions. For details about the recording process and both the recorded and simulated scenarios, see Appendix B.

Granular material	**Rec/Dynamo/Random**	**Sound sample**
Glass spheres with 2mm diameter	Simulation Dynamo	Sound sample 48
	Simulation random	Sound sample 63
	Recording	Sound sample 20
Glass spheres with 1mm diameter	Simulation Dynamo	Sound sample 43
	Simulation random	Sound sample 58
	Recording	Sound sample 13
Plastic discs with 4mm diameter	Simulation Dynamo	Sound sample 53
	Simulation random	Sound sample 68
	Recording	Sound sample 34

Table 6.6: Results from the sound simulation of random solid object collisions.

Granular material	**Solid material**	**Sound sample**
Glass spheres with 2mm diameter	Ceramic	Sound sample 64
	Metal	Sound sample 65
Glass spheres with 1mm diameter	Ceramic	Sound sample 59
	Metal	Sound sample 60
Plastic discs 4mm diameter	Ceramic	Sound sample 69
	Metal	Sound sample 72

Table 6.7: Comparison between simulated and recorded sounds of both the granular collisions and the solid objects collisions.

Scenario	**Rec/Dynamo/Random**	**Sound sample**
Glass spheres with 2mm diameter and ceramic cup	Simulation Dynamo	Sound sample 51
	Simulation random	Sound sample 66
	Recording	Sound sample 15
Glass spheres with 2mm diameter and metal cup	Simulation Dynamo	Sound sample 52
	Simulation random	Sound sample 67
	Recording	Sound sample 17
Glass spheres with 1mm diameter and ceramic cup	Simulation Dynamo	Sound sample 46
	Simulation Random	Sound sample 61
	Recording	Sound sample 8
Glass spheres with 1mm diameter and metal cup	Simulation Dynamo	Sound sample 47
	Simulation random	Sound sample 62
	Recording	Sound sample 10
Plastic discs with 4mm diameter and ceramic cup	Simulation Dynamo	Sound sample 56
	Simulation random	Sound sample 71
	Recording	Sound sample 29
Plastic discs with 4mm diameter and metal cup	Simulation dynamo	Sound sample 57
	Simulation random	Sound sample 70
	Recording	Sound sample 31

7. Conclusion

A granular material is formed by enormous amount of particles. The interactions between the particles are responsible not only for the visual behaviour of the granular material, but also for the sound the material produces. The goal of this thesis is to investigate the possibility of creating a method for sound simulation of granular materials.

We identified two sound producing phenomena connected with the granular materials:

- Solid objects collisions - the collisions between the particles of the granular material and the surrounding solid body objects.
- Granular collisions - the collisions among between the particles of the granular materials.

We used previous work of researchers in sound simulation of solid objects and showed that it can be successfully used for the collisions between solid objects and particles of granular materials. In case of the granular collisions, we approximated the sound of each collision as an acceleration noise produced by a pair of colliding elastic spheres. We verified that the method is capable of producing believable sounds of granular materials.

We also presented a probabilistic approach towards the random generation of the collision data. Presented probabilistic approach can be used to generate both the granular and the solid objects collisions. We showed that random collisions are a viable way for sound simulation of granular materials. The probabilistic approach is important, due to the fact that, most of the methods for visual simulation of granular materials don't provide the information about the particle collisions.

Admittedly, the current state of our method still has various limitations and open issues. On the other hand, from the beginning our aim was to make a first step towards a method for sound simulation of granular materials. We demonstrated that there is a way for sound simulation of granular material, that uses the data from visual simulation and produces corresponding audio.

7.1 Limitations and future work

In the presented method, each granular collision is treated independently. It means that we evaluate the acoustic pressure as if the collision occurred in isolation from the other particles. However, the presence of the other particles and solid objects may have an effect on the sound wave propagation. Solution of this problem remains an open question.

We presented a method for the synthesis of sounds produced by granular material. The input of this method is the granular collisions data. In other words, the list of all collisions that occur in the simulation. The data can be extracted directly from the simulation of granular material, or it can be randomly generated. We tested method using data from event driven simulation.

However, other methods for simulation of granular materials (using both the discrete and the continuum approach) don't provide the information about the granular collisions. In the continuum approach methods, there are no collisions computed. For such methods, the randomly generated collision data would seem appropriate. However, the question of reconstruction of local probability density function from the data provided by these methods remains open.

We propose the following idea, that would make use of data driven simulation approach:

1. We need to determine a high level description of the situation inside a window/cell. For example, such high level description might contain following information:

   - the portion of the window/cell that is filled with the granular material
   - mean particle velocity in the window/cell
   - variance of particle velocity in the window/cell
   - etc.

   We stress that, this description should be extractable from wide variety of simulation methods. We speculate that the high level description will contain information that correlate with the properties of the collisions: time of occurrence, location, normal, velocity.

2. When the high level description is defined, it also defines the domain of the window cells. In other words, we know all possible condition of the window/cells. We can discretely split this domain and for each window/cell condition generate the corresponding event driven simulation. From event driven simulation, we obtain information about the collisions, which we can use to reconstruct local PDF for the window/cell. We do this for all possible conditions of window/cells and thus obtain the PDF for each possible window/cell. These density functions create a databank that will be used in the sound simulation process.

3. We run the simulation of granular material using any method (discrete or continuous). From the simulation, we extract the high level description of the window/cells. For each window/cell, we use the databank and retrieve the PDF. The PDF is then used to generate random granular collision data.

The idea is summarised in Figure 7.1. If it is successful, a similar approach could be used also for collisions between the granular material and solid objects.

We used method for sound simulation of solid body collisions originally developed by O'Brien et al. [37]. Although the method is capable of producing high quality sounds, the results are only approximate. The method doesn't solve the sound wave propagation problem. However, there are methods capable of solving the sound wave propagation (see for example [22]). In our approach we are only modelling external forces from the collision between particles and the solid objects. By substituting O'Brien's method for a more sophisticated one, we should be able to receive physically correct results.

In our approach we omitted the damping of the solid objects caused by the presence of granular material. Listen to Recording 41 and Recording 42 of a

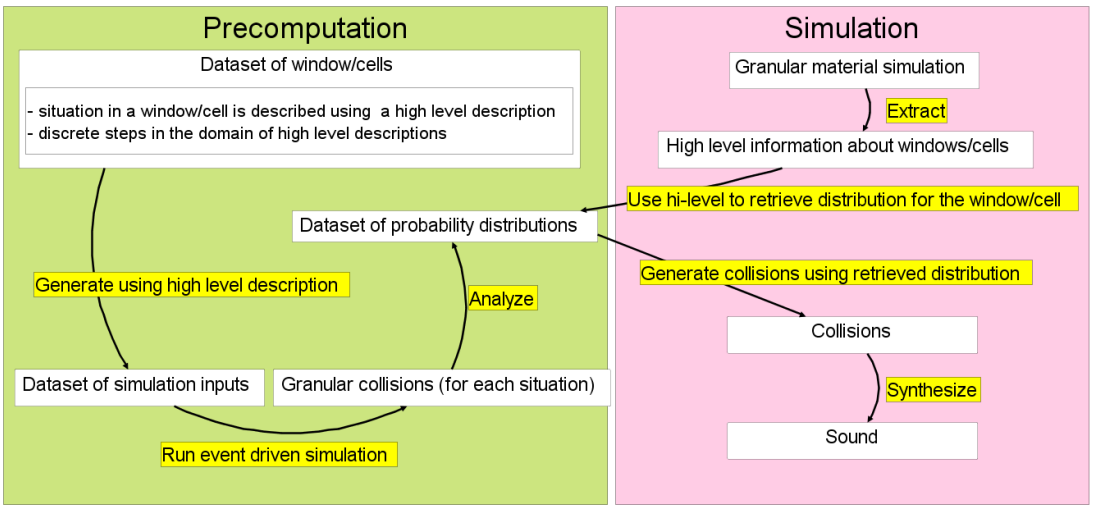

Figure 7.1: Idea for the future work: random granular collisions using a data driven simulation.

metal cup. In these recordings, the metal cup is filled with a granular material and empty respectively. The effect of damping is significant. The damping can be approximated by using different material of the cup in the simulation. However, more sophisticated approach is needed for a method that simulates sound of granular materials in an automatic way.

Bibliography

[1] Iván Alduán, Ángel Tena, and Miguel A. Otaduy. Simulation of high-resolution granular media. In *Proc. of Congreso Español de Informática Gráfica*, 2009.

[2] Steven S. An, Doug L. James, and Steve Marschner. Motion-driven concatenative synthesis of cloth sounds. *ACM Trans. Graph.*, 31(4):102:1–102:10, July 2012.

[3] M. N. Bannerman, R. Sargant, and L. Lue. Dynamo: a free O(n) general event-driven molecular dynamics simulator. *Journal of Computational Chemistry*, 32(15):3329–3338, 2011.

[4] Durand R. Begault. *3D Sound for Virtual Reality and Multimedia*. National Aeronautics and Space Administration, 2000. NASA technical memorandum version, available at `http://ntrs.nasa.gov/archive/nasa/casi.ntrs.nasa.gov/20010044352_2001071187.pdf`.

[5] Nathan Bell, Yizhou Yu, and Peter J. Mucha. Particle-based simulation of granular materials. In *Eurographics/ACM SIGGRAPH Symposium on Computer Animation*, 2005.

[6] Ilia Bisnovatyi. Flexible software framework for modal synthesis. In *Proceedings of the COST G-6 Conference on Digital Audio Effects (DAFX-00)*, 2000.

[7] R. Bridson. *Fluid Simulation For Computer Graphics*. A K PETERS Limited (MA), 2008.

[8] Michel Bruneau. *Fundamentals of Acoustics*. ISTE Ltd, 2006.

[9] N. Castagne and C. Cadoz. Genesis: A friendly musician-oriented environment for mass-interaction physical modeling. In *International Computer Music Conference*, 2002.

[10] Jeffrey N. Chadwick, Steven S. An, and Doug L. James. Harmonic shells: a practical nonlinear sound model for near-rigid thin shells. *ACM Trans. Graph.*, 28(5):119:1–119:10, December 2009.

[11] Jeffrey N. Chadwick and Doug L. James. Animating fire with sound. *ACM Trans. Graph.*, 30(4):84:1–84:8, July 2011.

[12] Jeffrey N. Chadwick, Changxi Zheng, and Doug L. James. Faster acceleration noise for multibody animations using precomputed soundbanks. *ACM/Eurographics Symposium on Computer Animation*, 2012.

[13] Jeffrey N. Chadwick, Changxi Zheng, and Doug L. James. Precomputed acceleration noise for improved rigid-body sound. *ACM Transactions on Graphics (Proceedings of SIGGRAPH 2012)*, 31(4), August 2012.

[14] Perry R. Cook. Physically informed sonic modeling (phism): Percussive synthesis. In *Proceedings of the International Computer Music Conference*, pages 228 – 231, 1996.

[15] Kees van den Doel. Physically based models for liquid sounds. *ACM Trans. Appl. Percept.*, 2(4):534–546, October 2005.

[16] William W. Gaver. How do we hear in the world? Explorations in ecological acoustics. *Ecological Psychology*, 5:285–313, 1993.

[17] William W. Gaver. Synthesizing auditory icons. In *Proceedings of the INTERACT '93 and CHI '93 Conference on Human Factors in Computing Systems*, CHI '93, pages 228–235, New York, NY, USA, 1993. ACM.

[18] William W. Gaver. What in the world do we hear? An ecological approach to auditory event perception. *Ecological Psychology*, 5:1–29, 1993.

[19] Jimin He and Zhi-Fang Fu. *Modal Analysis*. Butterworth-Heinemann, 2001.

[20] M. Ihmsen et al. A lagrangian framework for simulating granular material with high detail. *Computers & Graphics*, 2013.

[21] Finn Jacobsen, Torben Poulsen, Jens Holger Rindel, Anders Christian Gade, and Mogens Ohlrich. Fundamentals of acoustics and noise control, 2011. Lecture notes: `http://web-files.ait.dtu.dk/fjac/p_home_page/notes/Fundamentals_of_acoustics.pdf`.

[22] Doug L. James, Jernej Barbič, and Dinesh K. Pai. Precomputed acoustic transfer: output-sensitive, accurate sound generation for geometrically complex vibration sources. *ACM Trans. Graph.*, 25(3):987–995, July 2006.

[23] L.E. Kinsler. *Fundamentals of acoustics*. Wiley, 2000.

[24] L.L. Koss. Transient sound from colliding spheres—inelastic collisions. *Journal of Sound and Vibration*, 36(4):555 – 562, 1974.

[25] L.L. Koss and R.J. Alfredson. Transient sound radiated by spheres undergoing an elastic collision. *Journal of Sound and Vibration*, 27(1):59 – 75, 1973.

[26] Adam Lake. *Game Programming Gems 8*. Course Technology Press, Boston, MA, United States, 1st edition, 2010.

[27] T.G. Leighton. *The Acoustic Bubble*. Academic Press, 1994.

[28] Annie Luciani, Nicolas Castagne, and Nicolas Tixier. Metabolic emergent auditory effects by means of physical particle modeling: The example of musical sand. In *6th Int. Conference on Digital Audio Effects (DAFX-03)*, September 2003.

[29] K. Mehraby, H. Khademhosseini Beheshti, and M. Poursina. Impact noise radiated by collision of two spheres: Comparison between numerical simulations, experiments and analytical results. *Journal of Mechanical Science and Technology*, 25:1675–1685, 2011.

[30] Anita Mehta. *Granular physics*. Cambridge University Press, 2007.

[31] Chirag Mehta. Real-time synthesis of footfall sounds on sand and snow, and wood. Available online at `http://chir.ag/493/`, 2004.

[32] Marcel Minnaert. On musical air-bubbles and the sounds of running water. *Phil. Mag.*, 1933.

[33] William Moss, Hengchin Yeh, Jeong-Mo Hong, Ming C. Lin, and Dinesh Manocha. Sounding liquids: Automatic sound synthesis from fluid simulation. *ACM Trans. Graph.*, 29(3):21:1–21:13, July 2010.

[34] Rahul Narain, Abhinav Golas, and Ming C. Lin. Free-flowing granular materials with two-way solid coupling. *ACM Trans. Graph.*, 29(6):173:1–173:10, December 2010.

[35] James F. O'Brien, Perry R. Cook, and Georg Essl. Synthesizing sounds from physically based motion. In *Proceedings of ACM SIGGRAPH 2001*, pages 529–536. ACM Press, August 2001.

[36] James F. O'Brien and Jessica K. Hodgins. Graphical modeling and animation of brittle fracture. In *Proceedings of ACM SIGGRAPH 1999*, pages 137–146. ACM Press/Addison-Wesley Publishing Co., August 1999.

[37] James F. O'Brien, Chen Shen, and Christine M. Gatchalian. Synthesizing sounds from rigid-body simulations. In *The ACM SIGGRAPH 2002 Symposium on Computer Animation*, pages 175–181. ACM Press, July 2002.

[38] Dinesh K. Pai, Kees van den Doel, Doug L. James, Jochen Lang, John E. Lloyd, Joshua L. Richmond, and Som H. Yau. Scanning physical interaction behavior of 3D objects. In *Proceedings of the 28th annual conference on Computer graphics and interactive techniques*, SIGGRAPH '01, pages 87–96, New York, NY, USA, 2001. ACM.

[39] A. Pentland and J. Williams. Good vibrations: modal dynamics for graphics and animation. *SIGGRAPH Comput. Graph.*, 23(3):207–214, July 1989.

[40] Matt Pharr and Greg Humphreys. *Physically Based Rendering, Second Edition: From Theory To Implementation*. Morgan Kaufmann Publishers Inc., San Francisco, CA, USA, 2nd edition, 2010.

[41] Cecile Picard, Francois Antipolis, Sophia Faure, George Drettakis, and Paul G. Kry. A robust and multi-scale modal analysis for sound synthesis. In *12th International Conference on Digital Audio Effects (DAFx-09)*.

[42] Nikunj Raghuvanshi and Ming C. Lin. Interactive sound synthesis for large scale environments. In *Proceedings of the 2006 symposium on Interactive 3D graphics and games*, I3D '06, pages 101–108, New York, NY, USA, 2006. ACM.

[43] Inder K. Rana. From geometry to linear algebra: An introduction to linear algebra, 2006. Version from July 2013. Available at `http://www.mathresource.iitb.ac.in/linear%20algebra/`.

[44] E.J. Richards, M.E. Westcott, and R.K. Jeyapalan. On the prediction of impact noise, I: Acceleration noise. *Journal of Sound and Vibration*, 62(4):547 – 575, 1979.

[45] Ahmed A. Shabana. *Theory of Vibration, Volume II: Discrete and Continuous Systems*. Springer-Verlag, 1991. Softcover reprint of the hardcover 1st edition 1991.

[46] Chen Shen, Kris K. Hauser, Christine M. Gatchalian, and James F. O'Brien. Modal analysis for real-time viscoelastic deformation. In *Proceedings of SIGGRAPH 2002, Technical Sketch*, July 2002.

[47] Paul Sholtz, Michael Bretz, and Franco Nori. Sound-producing sand avalanches. *Contemporary physics*, 38(5):329–342, 1997.

[48] Tapio Takala and James Hahn. Sound rendering. In *Proceedings of the 19th annual conference on Computer graphics and interactive techniques*, SIGGRAPH '92, pages 211–220, New York, NY, USA, 1992. ACM.

[49] Dennis T. Trexler and Wilton N. Melhorn. Singing and booming sand dunes of California and Nevada, 1986. Version from July 2013. Originally published in California Geology, available online at `http://www.schweich.com/sbdA.html`.

[50] Luca Turchet, Stefania Serafin, Smilen Dimitrov, and Rolf Nordahl. Physically based sound synthesis and controls of footsteps sound. In *13th Int. Conference on Digital Audio Effects (DAFx-10)*, September 2010.

[51] Cornelis Pieter van den Doel. *Sound Synthesis for Virtual Reality and Computer Games*. diploma thesis, The University of British Columbia, 1998. `http://www.cs.ubc.ca/~kvdoel/publications/thesis.pdf`.

[52] Kees van den Doel, Paul G. Kry, and Dinesh K. Pai. Foleyautomatic: physically-based sound effects for interactive simulation and animation. In *Proceedings of the 28th annual conference on Computer graphics and interactive techniques*, SIGGRAPH '01, pages 537–544, New York, NY, USA, 2001. ACM.

[53] L.A. Wood and K.P. Byrne. Acceleration noise generated by a random repeated impact process. *Journal of Sound and Vibration*, 88(4):489 – 499, 1983.

[54] Changxi Zheng and Doug L. James. Harmonic fluids. *ACM Trans. Graph.*, 28(3):37:1–37:12, July 2009.

[55] Changxi Zheng and Doug L. James. Toward high-quality modal contact sound. *ACM Transactions on Graphics (Proceedings of SIGGRAPH 2011)*, 30(4), August 2011.

[56] Yongning Zhu and Robert Bridson. Animating sand as a fluid. In *ACM SIGGRAPH 2005 Papers*, SIGGRAPH '05, pages 965–972, New York, NY, USA, 2005. ACM.

A. Modal oscillators

The value of j-th modal oscillator is given by Equation 3.11 as:

$$z_j = c_{j,1}e^{t\omega_j^+} + c_{j,2}e^{t\omega_j^-}$$

and the values of constants $c_{j,1}$ and $c_{j,2}$ in Equation 3.13 are:

$$c_{j,1} = \frac{2\Delta t g_j}{\omega_j^+ - \omega_j^-} \qquad\qquad c_{j,2} = \frac{2\Delta t g_i}{\omega_j^- - \omega_j^+}.$$

We use the meaning of $\omega_j^{\pm}$ mentioned in [37]: the real part is mode's damping parameter and the absolute value of the imaginary part is the frequency. Thus we can write:

$$\omega_j^{\pm} = d \pm if.$$

From now on we will be dealing with a single oscillator. Therefore, the value of j is fixed and we can safely leave out the subscript:

$$z = c_1 e^{t\omega^+} + c_2 e^{t\omega^-}.$$

We substitute the values of c_1 and c_2 and simplify:

$$z = \frac{2\Delta t g}{d + if - d + if}e^{t\omega^+} + \frac{2\Delta t g}{d - if - d - if}e^{t\omega^-} =$$

$$= 2\Delta t g[\frac{e^{t\omega^+}}{2if} + \frac{e^{t\omega^-}}{-2if}] = \Delta t g[\frac{e^{t\omega^+} - e^{t\omega^-}}{if}] =$$

$$= \frac{\Delta t g}{if}[e^{t(d+if)} - e^{t(d-if)}] = \frac{\Delta t g}{if}[e^{td}e^{itf} - e^{td}e^{-itf}] =$$

$$= \frac{\Delta t g}{if}e^{td}[e^{itf} - e^{-itf}]$$

$$= \frac{\Delta t g}{if}e^{td}[\cos(tf) + i\sin(tf) - \cos(-tf) - i\sin(-tf)]$$

$$= \frac{\Delta t g}{if}e^{td}[i\sin(tf) - i\sin(-tf)] = \frac{2\Delta t g}{f}e^{td}\sin(tf).$$

We see that the result is the same as in given Article [37]. Although the oscillator is formulated in complex domain, the results are always real. Therefore, we can safely use only the real part of the complex oscillators.

Raghuvanshi and Lin [42] stated that instead of oscillators' positions, the velocities should be evaluated. We now prove that even for the velocity of the oscillator the resulting value is always real. We obtain the formula for the velocity of the oscillators by taking the derivative the Equation 3.11 with respect to time.

We have already proven that Equation 3.11 is real. Therefore, its derivative is also a real function. For the sake of exercise, we prove it explicitly. Once again the value of j is fixed (we deal with a single fixed oscillator in the proof) and we don't have to write the subscript:

$$\dot{z} = c_1\omega^+ e^{t\omega^+} + c_2\omega^- e^{t\omega^-}.$$

We follow the similar steps as in previous proof to obtain:

$$\dot{z} = \frac{\Delta t g}{if}[\omega^+ e^{t\omega^+} - \omega^- e^{t\omega^-}] = \frac{\Delta t g}{if} e^{td}[\omega^+ e^{itf} - \omega^- e^{-itf}] =$$

$$= \frac{\Delta t g}{if} e^{td}[(d+if)(\cos(tf) + i\sin(tf)) -$$

$$- (d-if)(\cos(-tf) + i\sin(-tf))]$$

$$= \frac{\Delta t g}{if} e^{td}[d\cos(tf) + di\sin(tf) + if\cos(tf) + i^2 f\sin(tf) -$$

$$- d\cos(-tf) + di\sin(tf) + if\cos(tf) + -i^2 f\sin(tf)]$$

$$= \frac{\Delta t g}{if} e^{td}[2di\sin(tf) + 2if\cos(tf)] = \frac{2\Delta t g}{f} e^{td}[d\sin(tf) + f\cos(tf)]$$

Again, we can see that the result is a purely real formula. Thus we can evaluate the complex oscillator formula and use only the real part.

B. Sound samples

This thesis is accompanied by a number of sound samples, which can be found on the included CD. The samples are located in the `/wave` folder. There are two subfolders in the `/wave` folder:

- `/wave/Recordings` - contains the recordings of the experiments, that are used to validate the simulation approach,
- `/wave/Simulations` - contains the result of the sound simulations.

B.1 Recordings

The recording of the real world experiments are necessary to support (or disprove) the hypotheses and reasoning in this thesis, as well as, to validate simulation results, by comparing them with real world examples. We chose to record the sound caused by a granular material being poured into a container. More precisely, a funnel is placed approximately 10cm above the container. The hole of the funnel is blocked and the funnel is filled with a small amount of a granular material. The hole is then opened and the material pours into the container. See Figure B.4 for the setup of the experiment. The funnel is made of thick paper. A cloth is glued to the surface of the funnel, to minimise the influence of the funnel-material interactions on the resulting sound (see Figure B.3).

We used the scenario with multiple different granular materials and containers. For each combination of granular material and container, we conducted two experiments. In the first one, the container was empty. In the second one, small amount of the material was present in the container. A metal cup prepared for the second case with a granular material inside is showed in Figure B.6. These two case are distinguished with the suffixes `Empty` and `Full` in the file names of the recordings.

The `wave/Recordings` folder contains multiple subfolders. Each subfolder contains recordings of one material with a different containers. We used the following materials:

- `Glass2mm` - glass spheres with the diameter of $2 - 3$mm,
- `Glass1mm` - glass spheres with the diameter of 1mm,
- `Glass0.5` - glass spheres with the diameter of 0.5mm,
- `Metal1mm` - iron spheres with the diameter of 1mm,
- `Plastic4mm` - disk shaped plastic material with the diameter of 4mm,
- `Sand` - common dry sand.

Figure B.1: Granular materials used in the recordings. In the back row, there are three types of glass spheres with different diameters. In the front we can see iron spheres and plastic dics.

During the experiments we used four different containers:

- Ceramic - a common ceramic cup for tea or coffee,
- Metal - one litre metal cup, depicted in Figure B.4,
- Plastic - plastic bowl,
- Void - a special container created by attaching cloth to the plastic bowl. It is depicted in Figure B.5. The cloth created a pocket, in which we poured granular material. We used this approach to minimise influence of the container and obtain sound produced purely by collisions among the grains of granular material. Void material is used only with a small amount of material already placed into the cloth pocket (i.e. the "Full" option).

All recordings were made using Shure P58 microphone plugged into M-Audio Fast Track sound card. The software package we used to record and manipulate (i.e. cut) the recordings is Audacity.

Figure B.2: Solid containers used in the recordings.

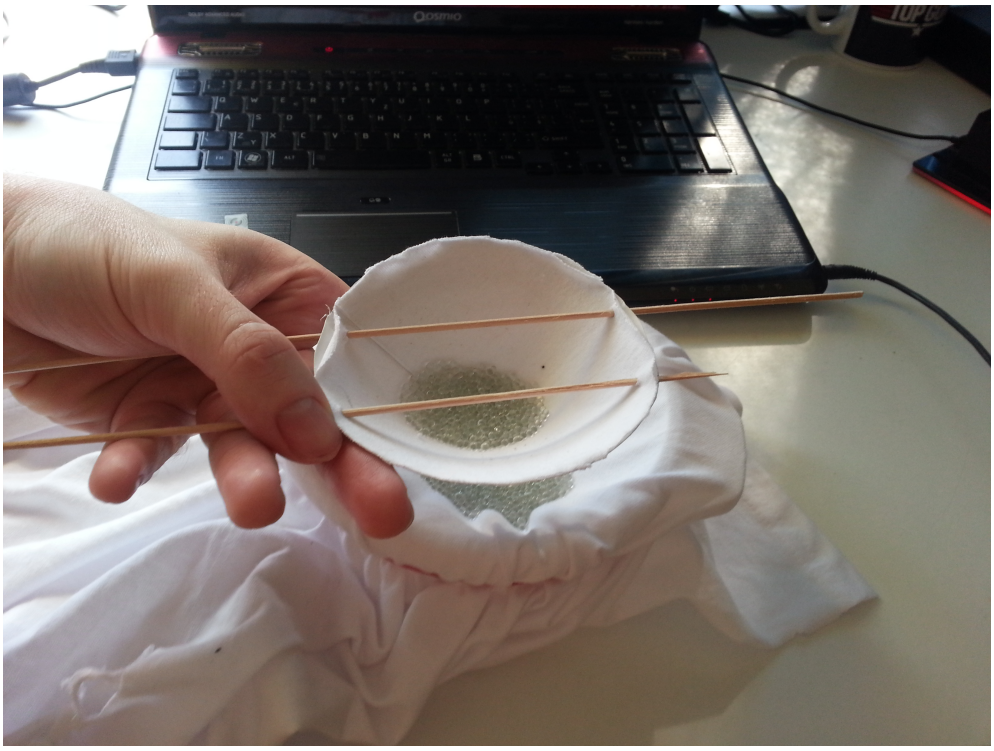

Figure B.3: The funnel used to obtain recordings. Notice the cloth layer glued to the funnel to minimise the sound produced by the interaction of granular material and the funnel.

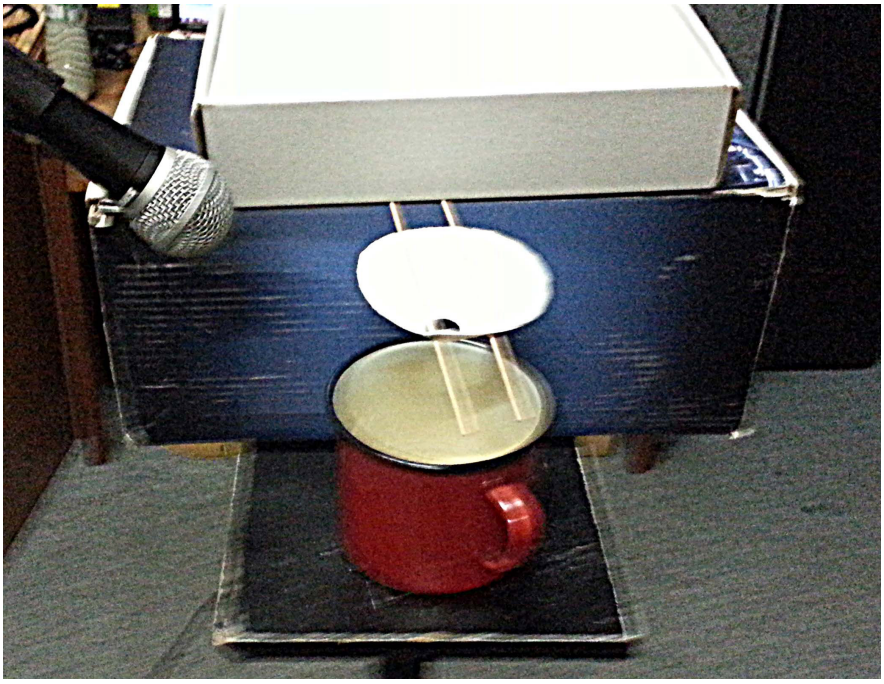

Figure B.4: The experimental setup used when recording the sound of granular materials. This particular case shows the metal cup underneath the funnel.

Figure B.5: Void material setup. A cloth is attached to a plastic bowl and the resulting pocket is filled with granular material. This approach is used to obtain sound caused purely by the collision of the grains.

Figure B.6: For each combination of granular material and container, we conducted one recording with a small amount of material already present in the container. This figure show a metal cup filled with plastic, disc-shaped particles of 4mm diameter.

Table B.1: List of experimental recordings. The files are located in the `/wave/Recordings` folder, in the subfolders that correspond with granular material used in the recording.

	Granular material	**Filename**
1	Glass0.5mm	CeramicEmpty.wav
2	Glass0.5mm	MetalEmpty.wav
3	Glass0.5mm	MetalFull.wav
4	Glass0.5mm	PlasticEmpty.wav
5	Glass0.5mm	PlasticFull.wav
6	Glass0.5mm	VoidFull.wav
7	Glass1mm	CeramicEmpty.wav

8	Glass1mm	CeramicFull.wav
9	Glass1mm	MetalEmpty.wav
10	Glass1mm	MetalFull.wav
11	Glass1mm	PlasticEmpty.wav
12	Glass1mm	PlasticFull.wav
13	Glass1mm	VoidFull.wav
14	Glass2mm	CeramicEmpty.wav
15	Glass2mm	CeramicFull.wav
16	Glass2mm	MetalEmpty.wav
17	Glass2mm	MetalFull.wav
18	Glass2mm	PlasticEmpty.wav
19	Glass2mm	PlasticFull.wav
20	Glass2mm	VoidFull.wav
21	Metal1mm	CeramicEmpty.wav
22	Metal1mm	CeramicFull.wav
23	Metal1mm	MetalEmpty.wav
24	Metal1mm	MetalFull.wav
25	Metal1mm	PlasticEmpty.wav
26	Metal1mm	PlasticFull.wav
27	Metal1mm	VoidFull.wav
28	Plastic4mm	CeramicEmpty.wav
29	Plastic4mm	CeramicFull.wav
30	Plastic4mm	MetalEmpty.wav
31	Plastic4mm	MetalFull.wav
32	Plastic4mm	PlasticEmpty.wav
33	Plastic4mm	PlasticFull.wav
34	Plastic4mm	VoidFull.wav
35	Sand	CeramicEmpty.wav
36	Sand	CeramicFull.wav
37	Sand	MetalEmpty.wav
38	Sand	MetalFull.wav
39	Sand	PlasticEmpty.wav
40	Sand	PlasticFull.wav

Table B.2: The influence of granular material on damping of solid objects' vibrations. Comparison of the sound produced by an empty metal cup and the same cup filled with a granular material. The files are located in the `/wave/Recordings/Damping` folder.

	Filename	**Description**
41	MetalFull.wav	Metal cup filled with granular material
42	MetalEmpty.wav	Empty metal cup

B.2 Simulations

The sound samples resulting from simulations are located in the `wave/Simulations` folder. The sounds are synthesised by simulating acceleration noise of the granular collisions (see Chapter 5). The collisions data is produced by the Dynamo[1] event driven simulator. We simulated a scenario similar to the one used in the recordings of the granular materials.

The scenario contains a cup and a funnel above formed by static particles. Desired amount of granular material is put inside the funnel (typically 500 or 1000 particles). During the simulation the particles fall down from funnel into the cup. Optionally, the cup may contain some granular material. The particles inside the cup have been previously simulated, until they achieved rest positions.

The scenario described above is very similar to the recorded real-world experiments. However, there is one difference. In the real world scenarios, the granular material in the funnel is at rest at the bottom of the funnel. In the simulations, the material is placed above the bottom of the funnel (i.e. "it is hanging in the air"). The simulations with the material resting at the bottom of the funnel proved to be problematic. The event driven simulation always advances time to the closest event, the closest particle collision in this case. The bottom of the funnel is very exposed place and enormous amount of collisions occurs there. With the material resting at the bottom, we have reached 10 million collisions without a single particle falling down from a funnel. Therefore, we decided to start the simulations with the granular material above the bottom. We simulate different scenario than the one being recorded. However, we assume that the pair is similar enough to allow us comparison of the overall characteristics of the sounds.

[1]Dynamo website can be found at `http://dynamomd.org/`. We used modified source code, that allows us to obtain necessary data about all collisions that occur during the simulation.

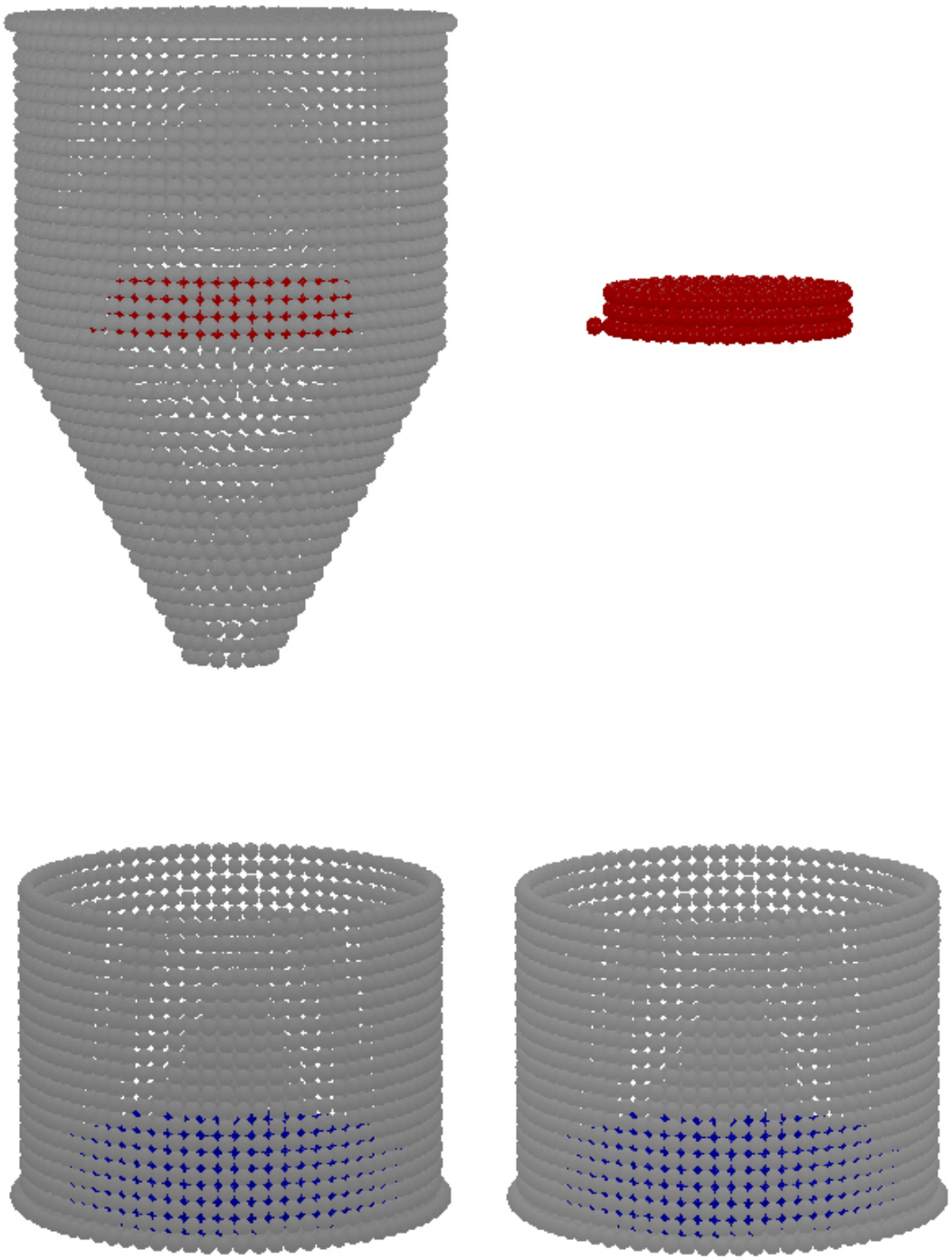

Figure B.7: Screenshot from Dynamo shows the simulation scenario used to obtain collision data. In the right picture, the funnel is not displayed. Notice the granular material in the funnel (the dark red particles), which is above the bottom of the funnel.

Table B.3: List of sound samples generated using collision data from Dynamo simulations. The files are located in the `/wave/Simulations` folder, in the subfolders that correspond with granular material used in the recording.

	Granular material	**Filename**	**Description**
43	Glass1mm	granularCollisions.wav	Granular collisions
44	Glass1mm	ceramicCollisions.wav	Solid objects collisions with a ceramic cup
45	Glass1mm	metalCollisions.wav	Solid objects collisions with a metal cup
46	Glass1mm	granularCeramic.wav	Granular collisions and solid objects collisions with a ceramic cup
47	Glass1mm	granularMetal.wav	Granular collisions and solid objects collisions with a metal cup
48	Glass2mm	granularCollisions.wav	Granular collisions
49	Glass2mm	ceramicCollisions.wav	Solid objects collisions with a ceramic cup
50	Glass2mm	metalCollisions.wav	Solid objects collisions with a metal cup
51	Glass2mm	granularCeramic.wav	Granular collisions and solid objects collisions with a ceramic cup
52	Glass2mm	granularMetal.wav	Granular collisions and solid objects collisions with a metal cup
53	Plastic4mm	granularCollisions.wav	Granular collisions
54	Plastic4mm	ceramicCollisions.wav	Solid objects collisions with a ceramic cup
55	Plastic4mm	metalCollisions.wav	Solid objects collisions with a metal cup
56	Plastic4mm	granularCeramic.wav	Granular collisions and solid objects collisions with a ceramic cup
57	Plastic4mm	granularMetal.wav	Granular collisions and solid objects collisions with a metal cup

Table B.4: List of sound samples generated using random collision data. The probability density function were reconstructed from collision data from Dynamo simulations. The files are located in the `/wave/Simulations` folder, in the subfolders that correspond with granular material used in the recording.

	Material	**Filename**	**Description**
58	Glass1mm	granularCollisionsRandom.wav	Granular collisions
59	Glass1mm	ceramicCollisionsRandom.wav	Solid objects collisions with a ceramic cup
60	Glass1mm	metalCollisionsRandom.wav	Solid objects collisions with a metal cup
61	Glass1mm	granularCeramicRandom.wav	Granular collisions and solid objects collisions with a ceramic cup
62	Glass1mm	granularMetalRandom.wav	Granular collisions and solid objects collisions with a metal cup
63	Glass2mm	granularCollisionsRandom.wav	Granular collisions
64	Glass2mm	ceramicCollisionsRandom.wav	Solid objects collisions with a ceramic cup
65	Glass2mm	metalCollisionsRandom.wav	Solid objects collisions with a metal cup
66	Glass2mm	granularCeramicRandom.wav	Granular collisions and solid objects collisions with a ceramic cup
67	Glass2mm	granularMetalRandom.wav	Granular collisions and solid objects collisions with a metal cup
68	Plastic4mm	granularCollisionsRandom.wav	Granular collisions
69	Plastic4mm	ceramicCollisionsRandom.wav	Solid objects collisions with a ceramic cup
70	Plastic4mm	granularMetalRandom.wav	Solid objects collisions with a metal cup
71	Plastic4mm	granularCeramicRandom.wav	Granular collisions and solid objects collisions with a ceramic cup
72	Plastic4mm	metalCollisionsRandom.wav	Granular collisions and solid objects collisions with a metal cup

We also include the list of the simulation results we used to determine the relative importance of the parameters of granular collisions. These samples were generated using the following approach. We used a granular collision data from Dynamo. We randomly modified the parameters of each collision. All of the samples in Table B.5 were generated using the same material: glass spheres with 1mm radius. The properties of the glass sphere are: density $\rho = 2520\mathrm{kg\,m^{-3}}$, Young's modulus $E = 72\mathrm{GPa}$ and Poisson's ratio $\nu = 0.22$. The sounds are located in the `/wave/simulations/importance` folder.

Table B.5: List of sound samples from simulations used to determine the importance of the granular collisions' parameters. The files are located in the `/wave/Simulations/Importance` folder.

	Filename	**Description**
73	NonRandomized.wav	Original collision data.
74	Positions0.01.wav	Random location within $1cm$ regular grid cells.
75	Positions0.02.wav	Random location within $2cm$ regular grid cells.
76	Normals.wav	Random normal direction.
77	Positions0.01Normals.wav	Random location within $1cm$ regular grid cells and random normal.
78	Positions0.02Normals.wav	Random location within $2cm$ regular grid cells and random normal.
79	NormalsV0Limit0.5.wav	Random normal direction for collisions with $v_0 < 0.5\mathrm{m\,s^{-1}}$. 45251 out of 46932 collisions were changed.
80	NormalsV0Limit1.0.wav	Random normal direction for collisions with $v_0 < 1.0\mathrm{m\,s^{-1}}$. 46618 out of 46932 collisions were changed.
81	Positions0.02NormalsV0Limit0.5.wav	Random position within $2cm$ regular grid cells and random normal direction for collisions with $v_0 < 0.5\mathrm{m\,s^{-1}}$.

C. CD contents

This thesis is accompanied by a CD that contains the following directories and files:

- `/src/GranularSound` - source codes, material definitions and models we used to generate the sounds in this thesis. The goal of the thesis was not to develop a stand alone application. Therefore, the code remains highly experimental and it requires multiple prerequisites (Intel's MKL library for instance). We don't guarantee that the code can be compiled in the form present on the CD.
- `/src/thesis` - LaTeXsources and figures data for this thesis.
- `/wave` - sound samples referenced in the thesis. For more details, see Appendix B.
- `/thesis.pdf` - electronic version of this document.